New Quasar Microlensing Constraints on the Spin of High Redshift Quasars

Xinyu Dai (University of Oklahoma)

Acknowledgement:

Postdocs: Bin Chen, Eduardo Guerras
Graduate Students: Shaun Steele, Burak Dogurel, Saloni Bhatiani, Brett Bonine
Collaborators: Chris Morgan, George Chartas, Chris Kochanek

Quasar Microlensing (equiv. nano-arcsec resolution)

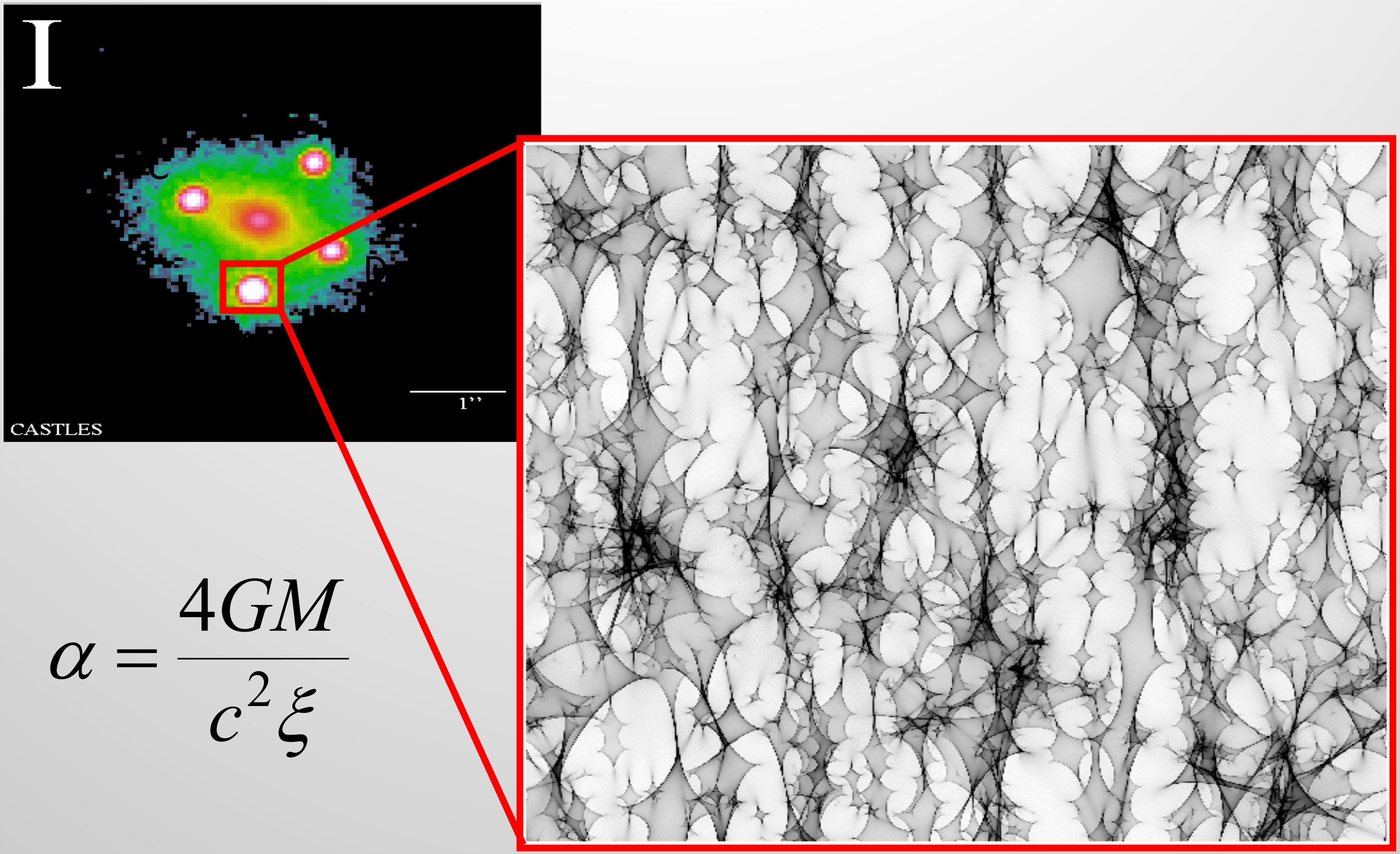

$$\alpha = \frac{4GM}{c^2 \xi}$$

Microlensing Light Curves Can Constrain Source Size

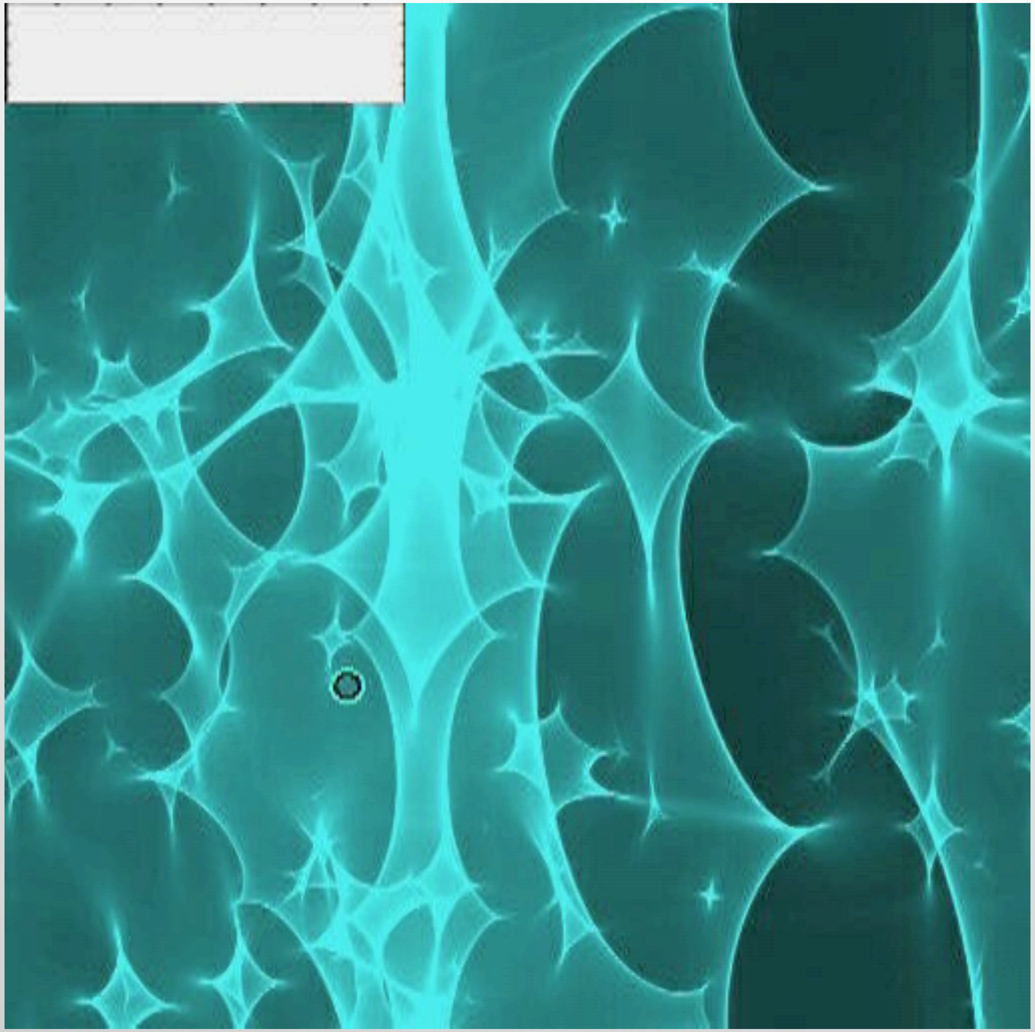

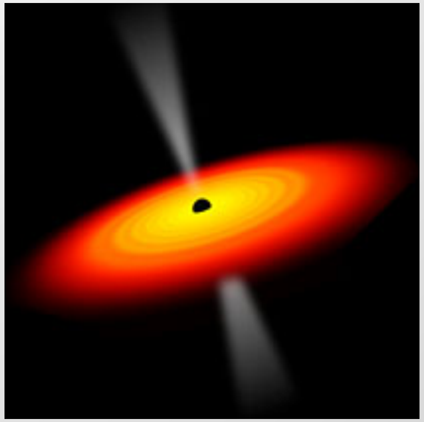

Large Source Size Smooth the Magnification Map and Have Smaller ML Variability

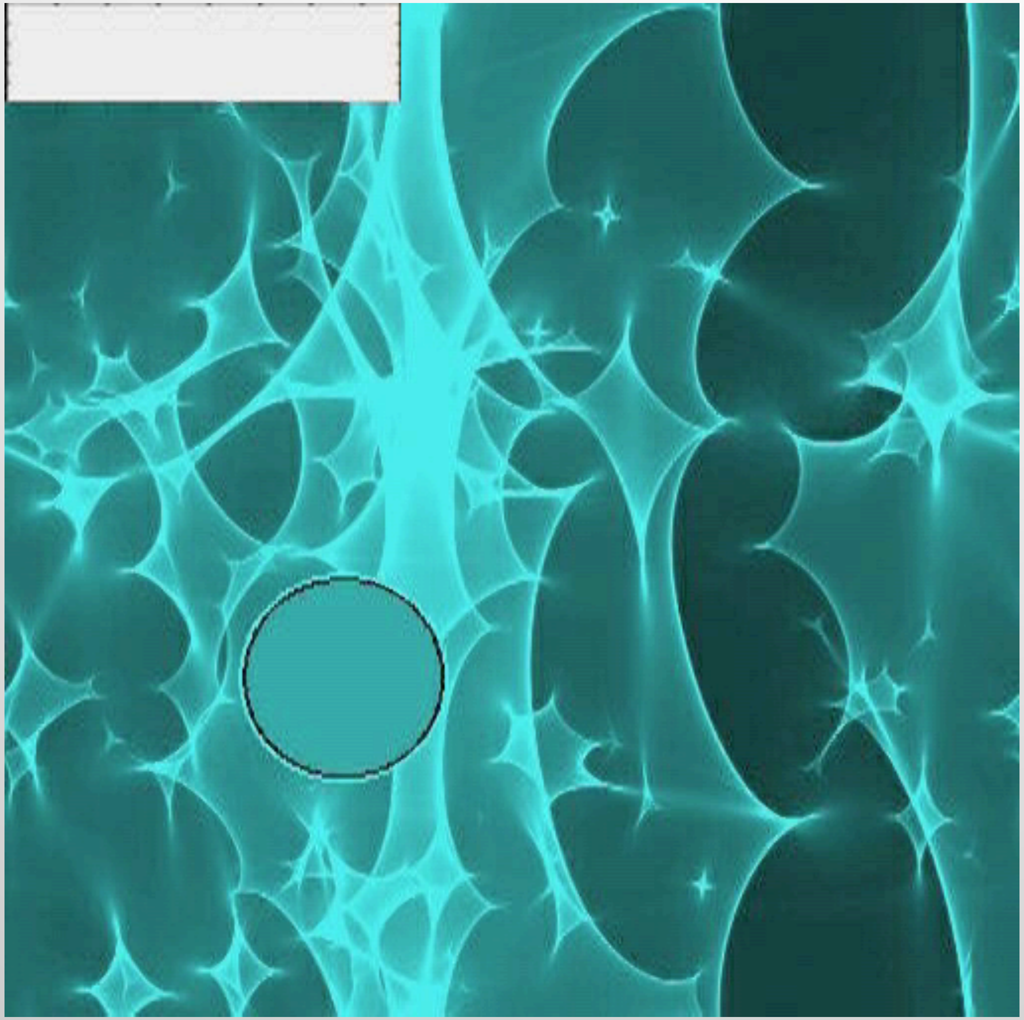

- Applied to ~10 targets
- Three Chandra LP programs (540 ks, 810 ks, and 885 ks)
- Ground-based Optical Monitoring with e.g., SMARTS, USNO, and other telescopes

What Can Quasar Microlensing Measure?

- Everything within Einstein Ring
- Broad line regions 😀😀😀
- Optical Continuum 😃😃
- X-ray Continuum 😁😁😁
- FeK region 😁😁😁
- Spin of Black Holes 👍👍
- Lens Population 😎😎😎
- Unresolved Jet on going

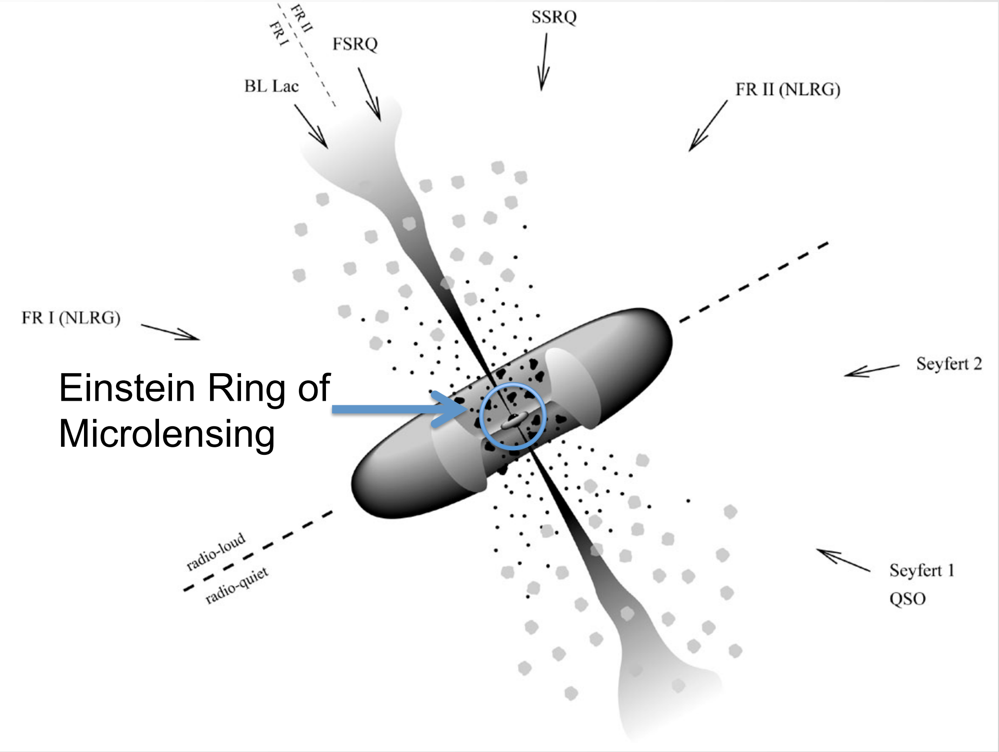

Einstein Ring of Microlensing

Measuring Quasar Microlensing Light Curves

A–B = 12.0, A–C = 9.6, A–D = –87 days

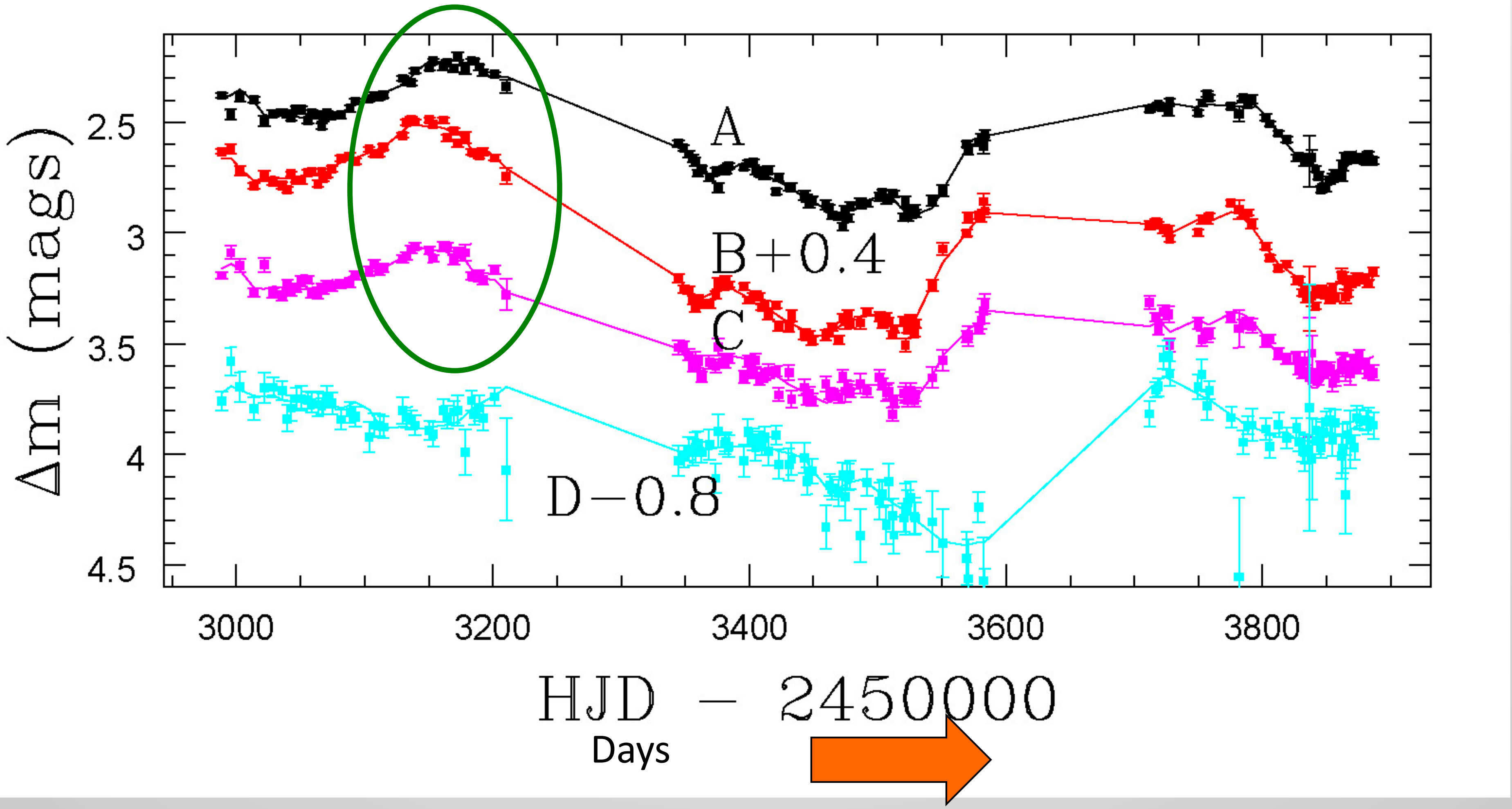

Shift and divide light curves –> Microlensing Variability

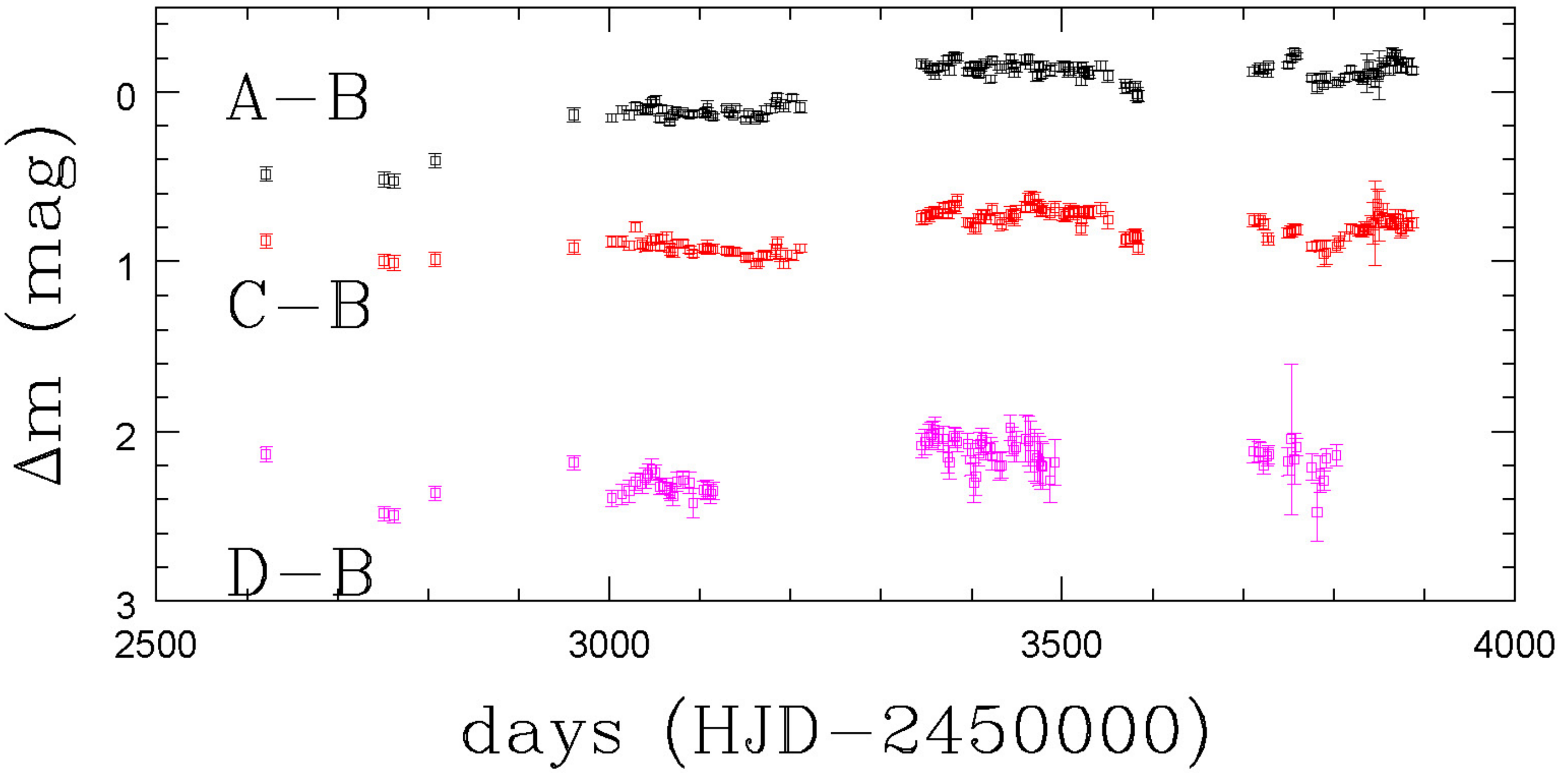

We observe this in almost all the systems we monitor

Analysis Methods

- Light curve fitting (Kochanek 2004 and later papers)
- Based on mean microlensing signal (e.g. Jiménez-Vicente+15, Guerras+17)
- Based on second moment of $\boldsymbol{\mu}$L light curve (RMS or modified RMS, e.g. Guerras+18)

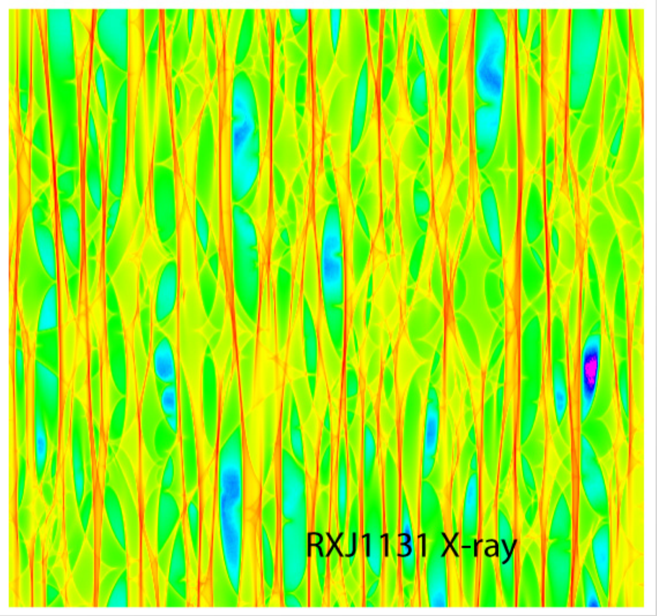

X-ray Corona and Reflection Component

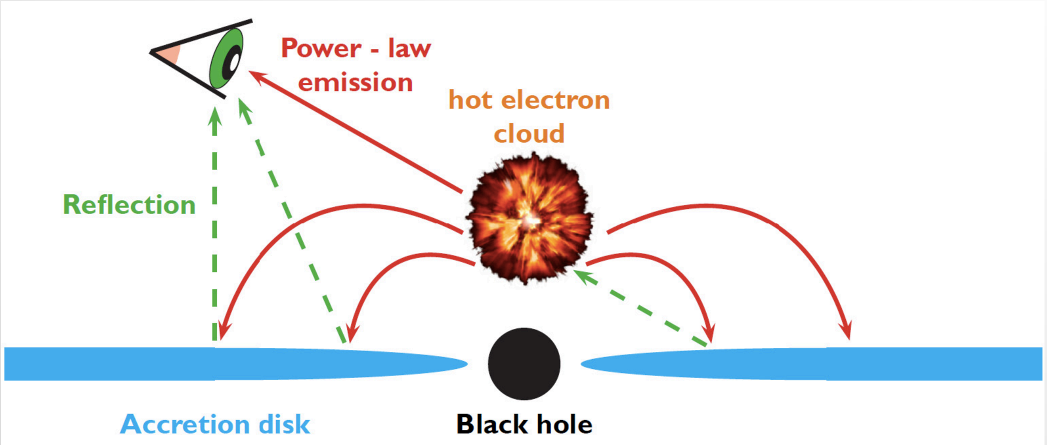

Credit: Athena Website

Chandra Band
For z = 1.5 quasar

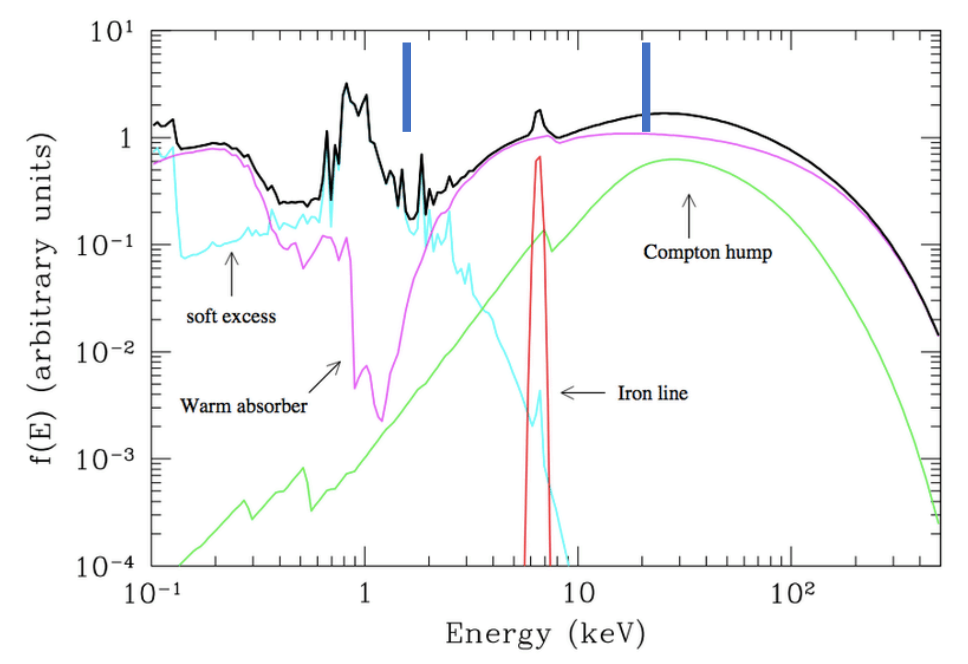

Risaliti & Elvis (2004)

X-ray Data (Chandra X-ray Observatory)

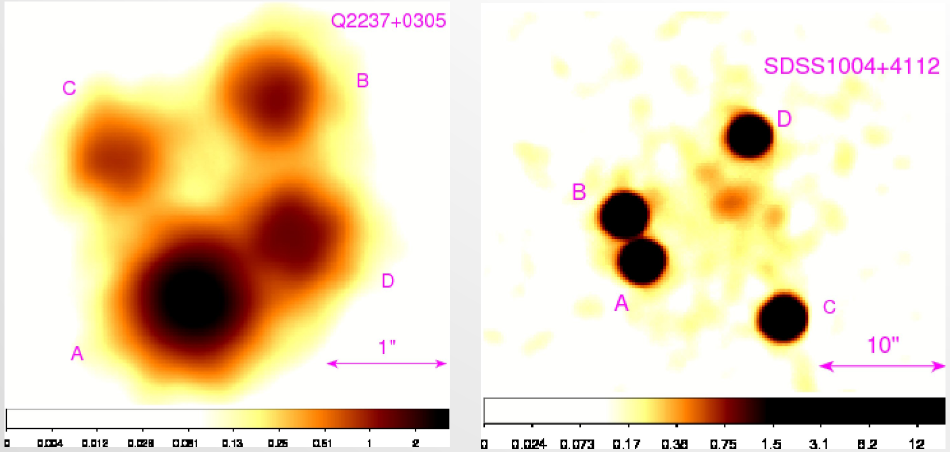

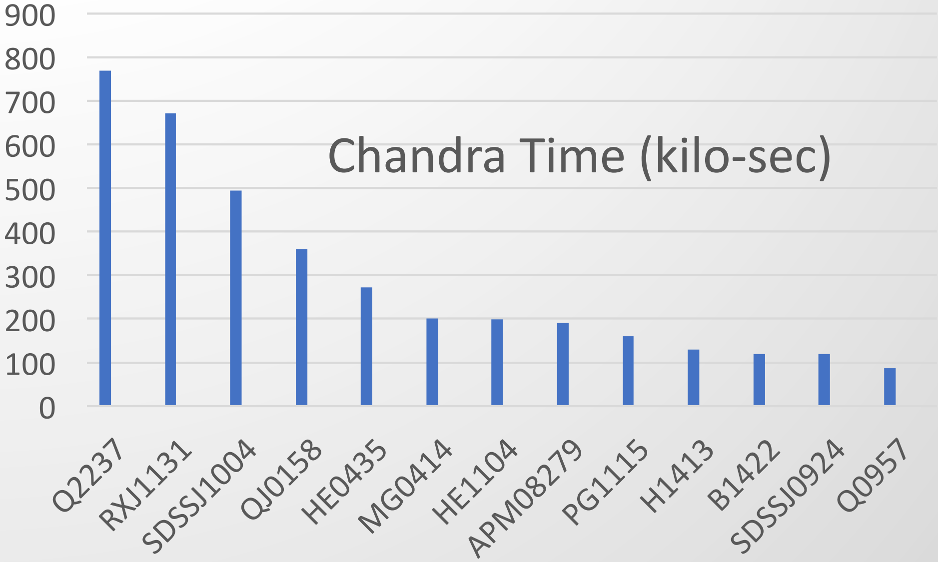

- ~30 lenses with total expo. of ~4.5 Ms
- Papers containing data: e.g. Guerras+2017, Chartas+2017, Dai+2019, Chen+2012, Blackburne+2011

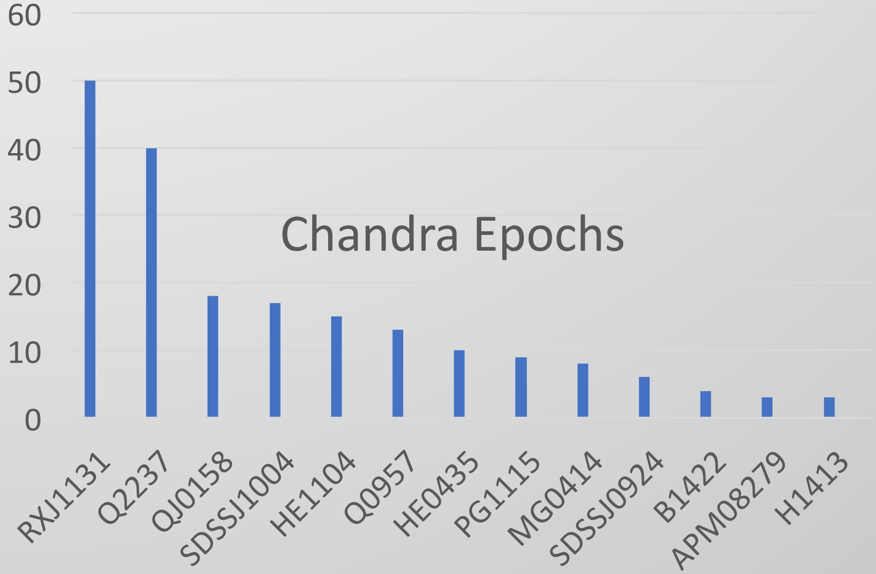

Example Optical and X-ray Microlensing Variability

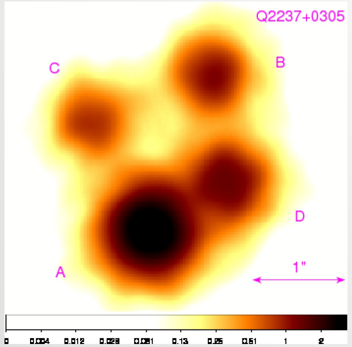

Q2237, Chen et al. (2011, 2012); Mosquera et al. (2013)

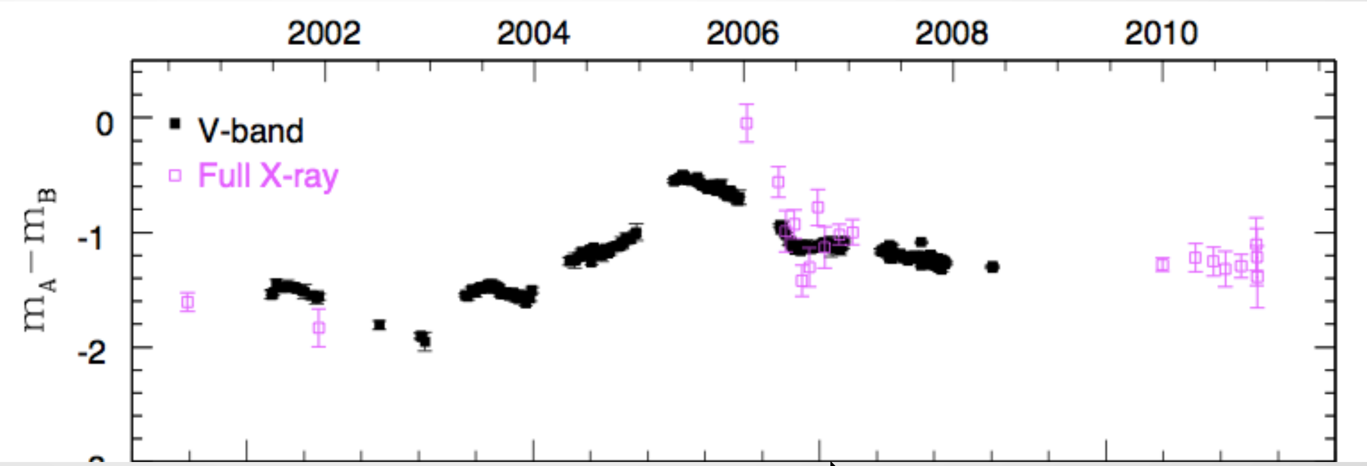

Time

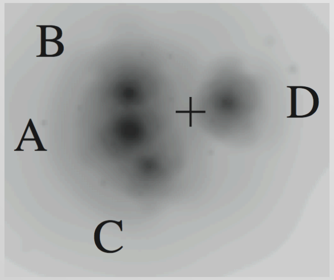

RXJ1131, Chartas et al. (2012)

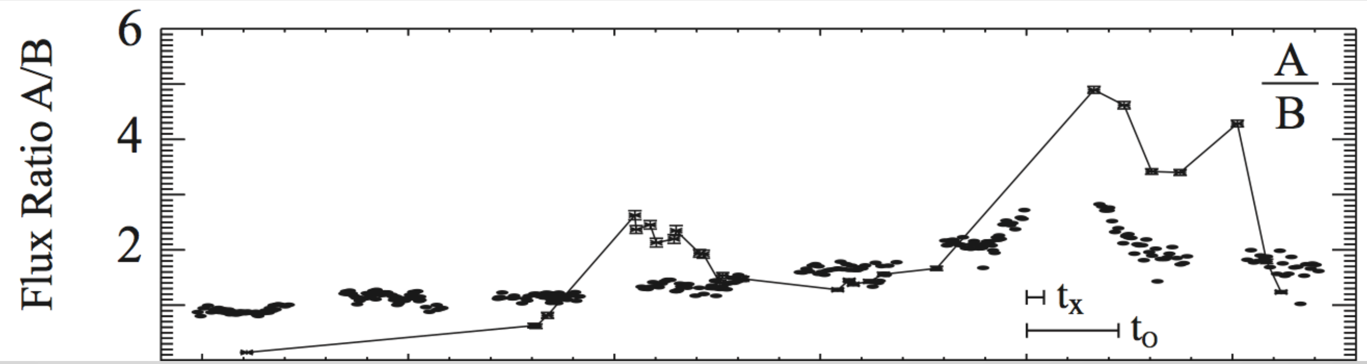

A Solution in RXJ1131-1231

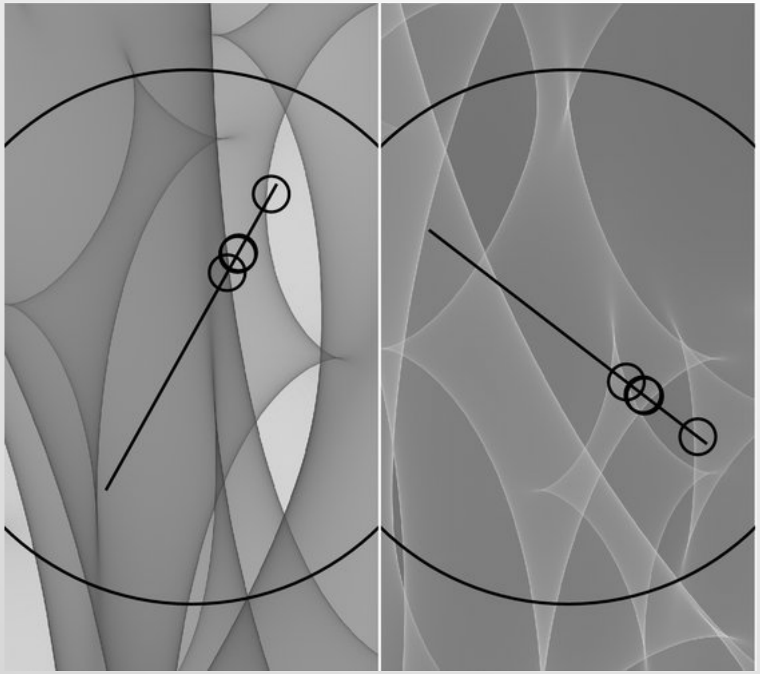

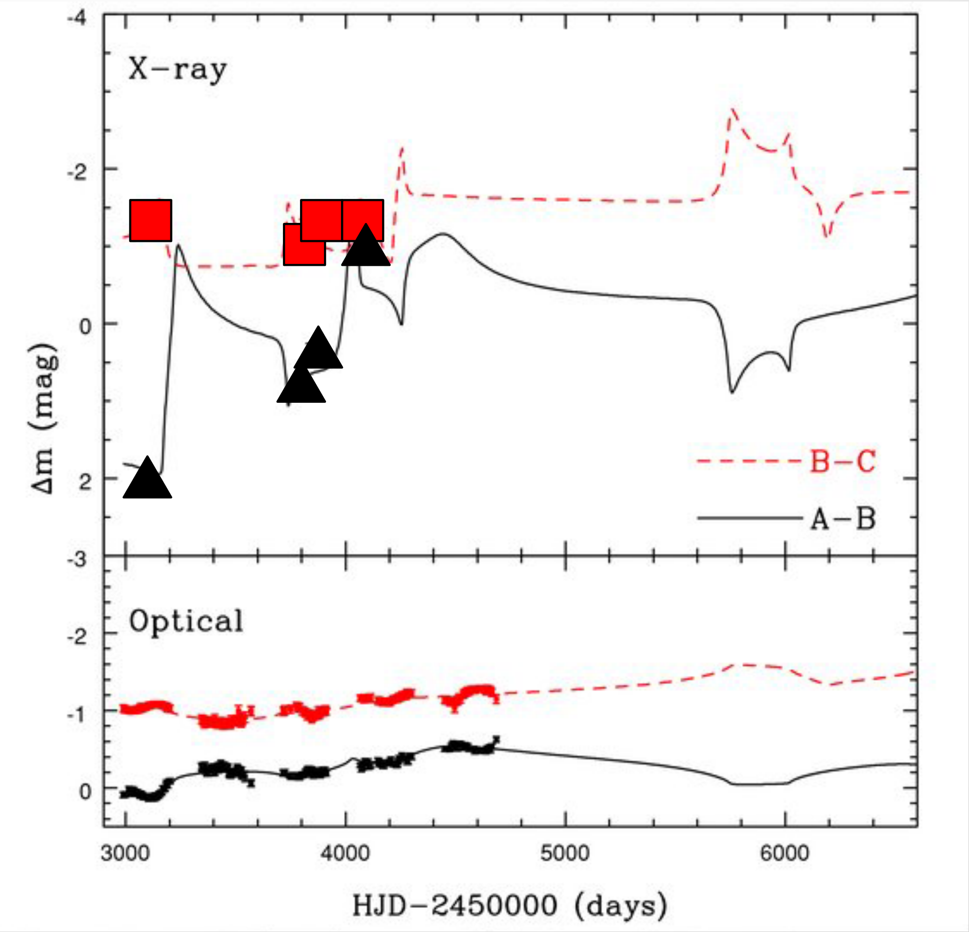

Dai et al. 2010, ApJ, 709, 278

X-ray and Optical Emission Sizes (Joint Optical-X-ray Analysis, Light Curve Fitting, Kochanek 2004)

Probability

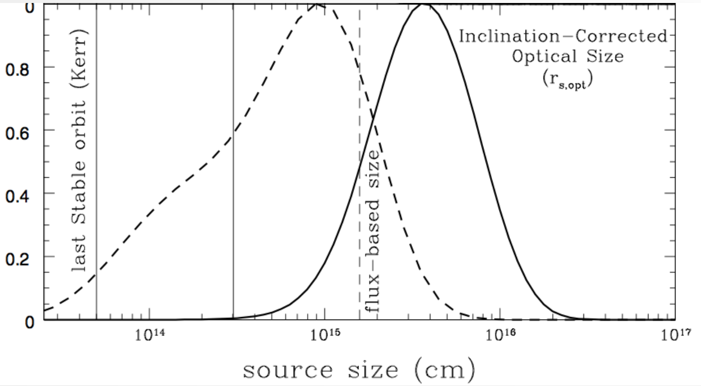

QJ0158, Morgan et al. (2012)

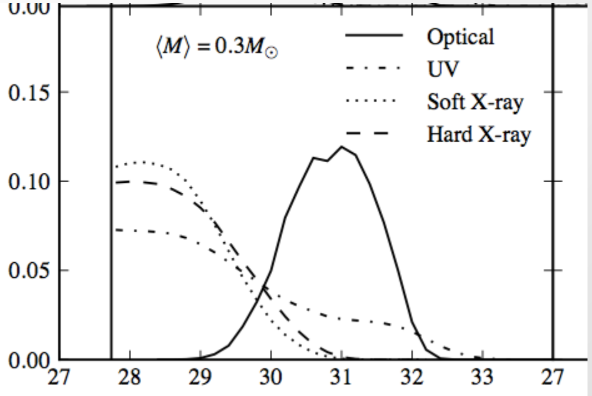

HE0435, Blackburne et al. (2011)

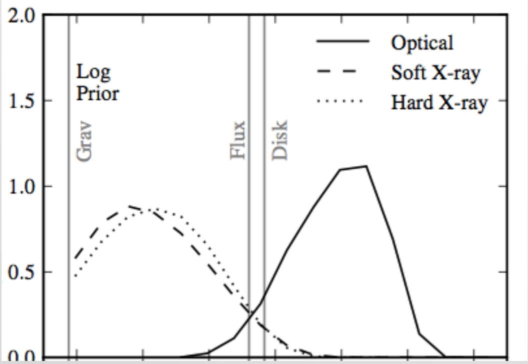

HE1104, Blackburne et al. (2013)

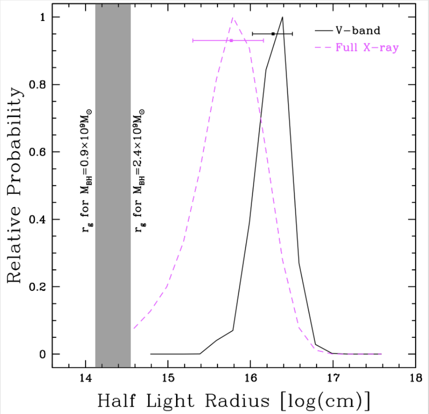

Q2237, Mosquera et al. (2013)

Morgan+2008 (PG1115),
Dai+2010 (RXJ1131)

Size

Optical bands: Challenge Thin Disk Models

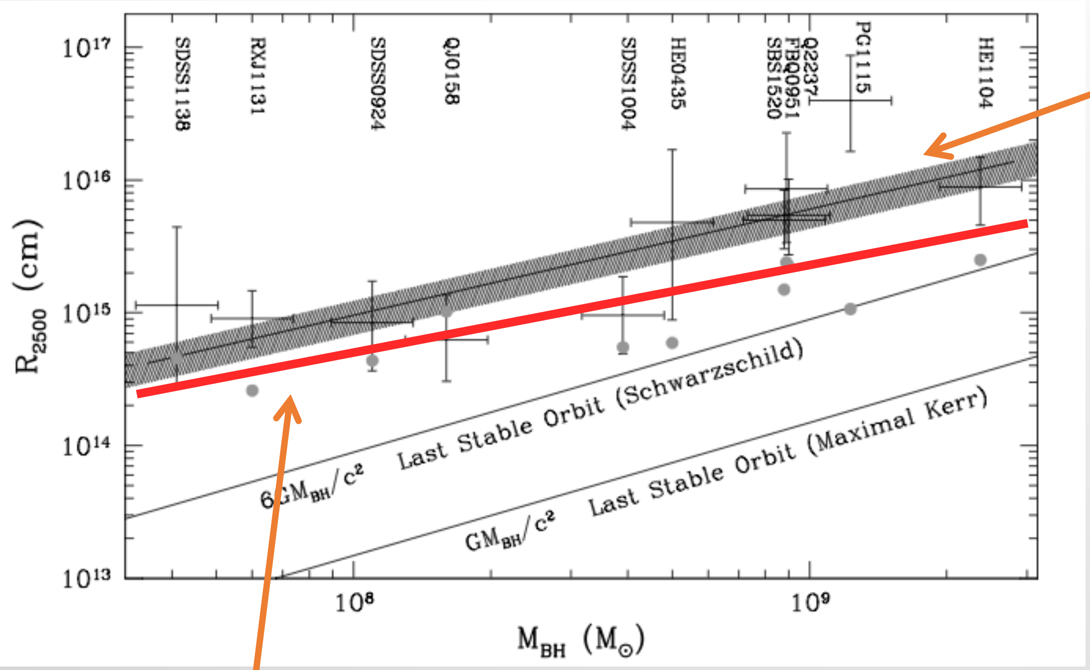

Microlensing

Thin Disk Prediction

- The classic thin disk model (Shakura & Sunyaev 1973) predicts

$$T \propto R^{-3/4}$$

- 2-3 times smaller than microlensing sizes (Dai+10, Morgan+10).
- Consistent Slope
- Confirmed by Reverberation Mapping method

AGN Wind Comes to Rescue (Li, Yuan, Dai 2019, also Sun+2019)

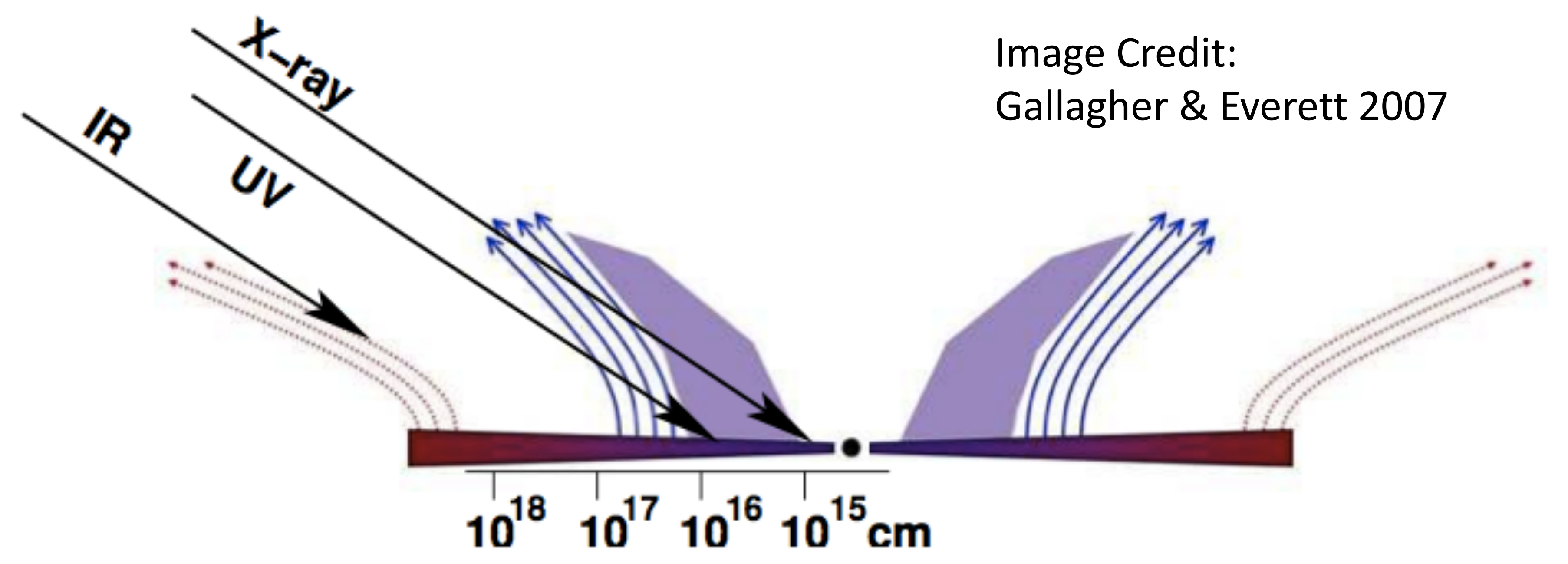

Image Credit:
Gallagher & Everett 2007

$T \propto R^{-(3-s)/4}$ S: Wind Strength

Wind Model for ***μ***L Disk Size Discrepancy (Li, Yuan, Dai 2019, Sun+2019)

$$\dot{M}(R) = \dot{M}_{\rm in}\left(\frac{R}{R_0}\right)^s, \quad R \geq R_0$$

$$R_{\lambda_0,{\rm th}}(\beta) = \left[\frac{45 f G^2 m_{\rm p} \lambda_0^4 M_{\rm BH}^2}{4\eta\pi^5 h_{\rm p} c^3 \sigma_{\rm T} R_0^s}\right]^{1/(3-s)}$$

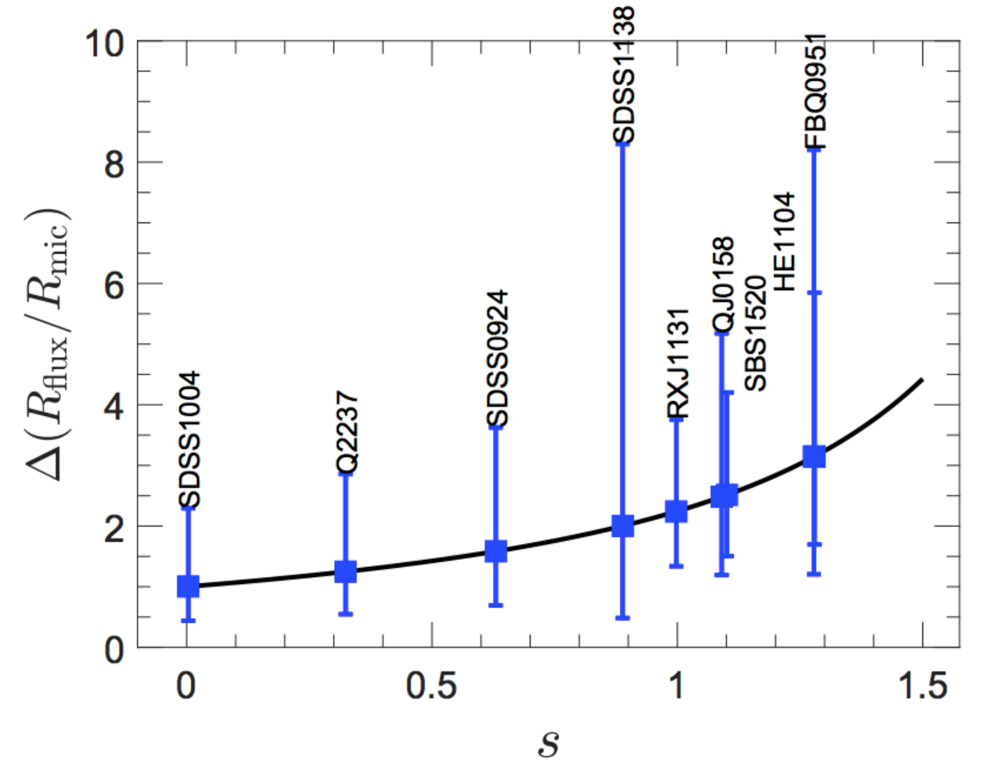

X-ray (~10-20 Rg, smallest 6Rg) and Scales with BH Mass

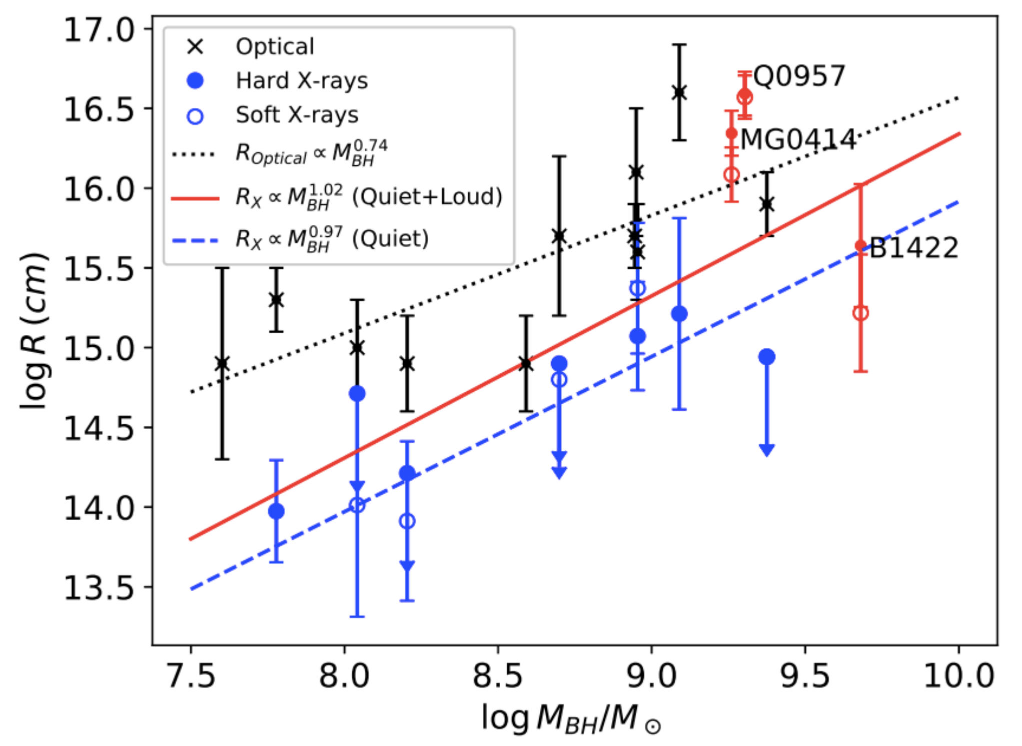

Dogruel et al. (2020), ApJ, 894, 153

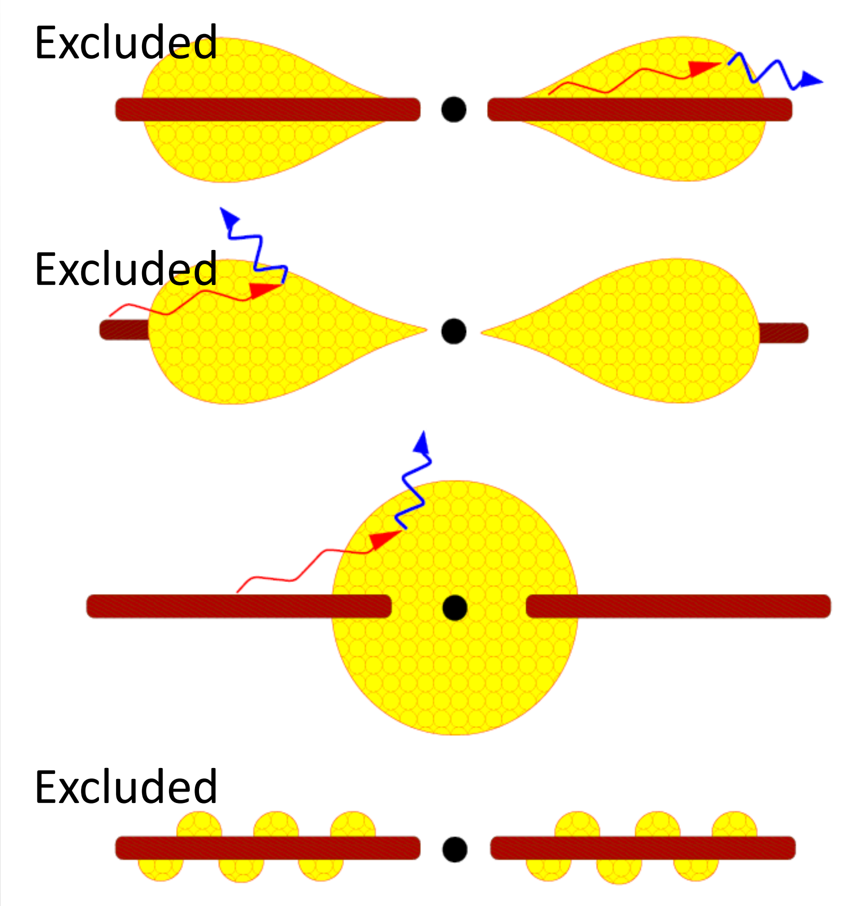

Reynolds & Nowak 2003 models

Relativistic Reflection Region

Reflection Region: Microlensing of Iron Lines (Chen et al. 2012, Chartas et al. 2017, Dai et al. 2019)

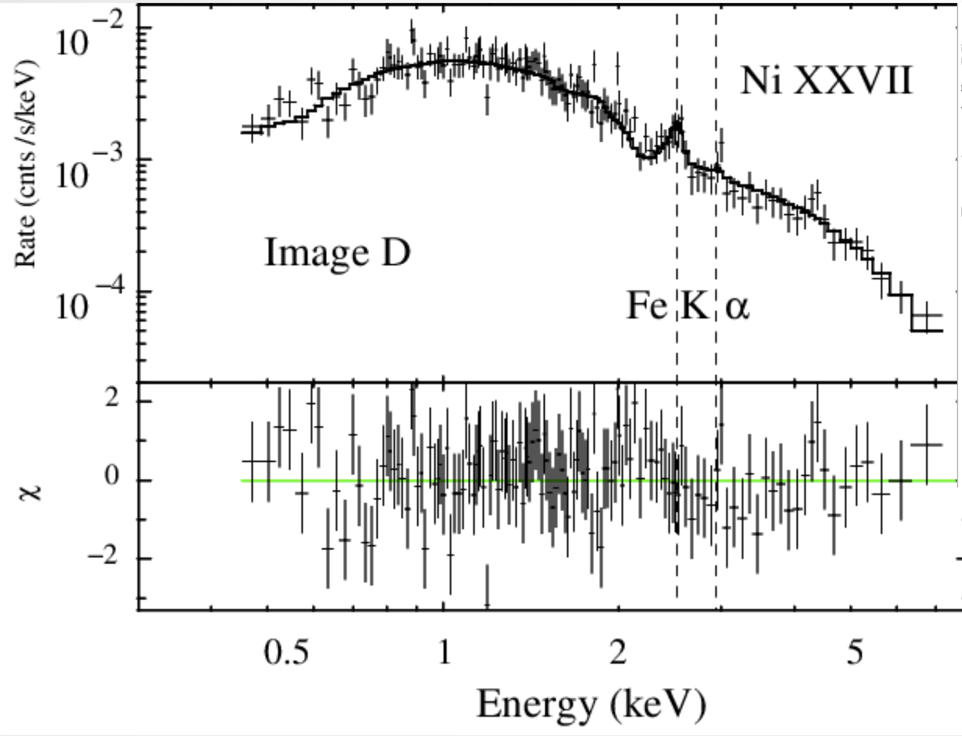

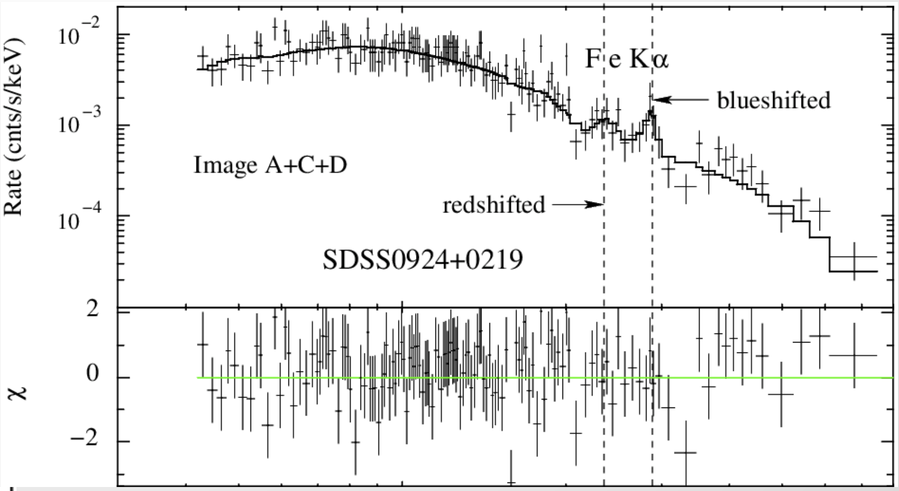

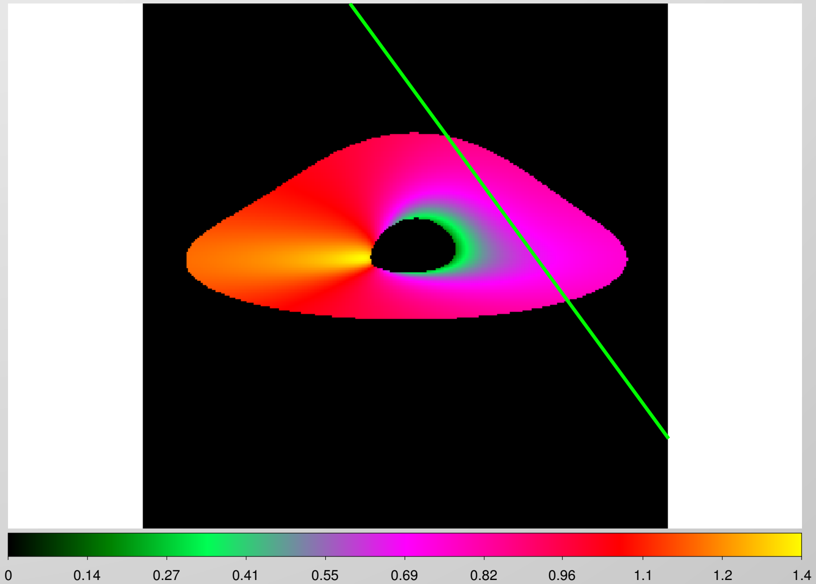

- Fe Lines are observed in almost all case.
- Sometime we see split of the line.

$\boldsymbol{\mu}$L Line Shift Simulations Papers

- Popović, Mediavilla, Jovanović, Muñoz, J. A. 2003
- Popović+2006
- Chartas+2017
- Ledvina, Heyrovský, Dovčiak 2018
- Krawczynski & Chartas 2018
- Krawczynski, Chartas, Kislat2019

Microlensing Analysis of the Iron Lines

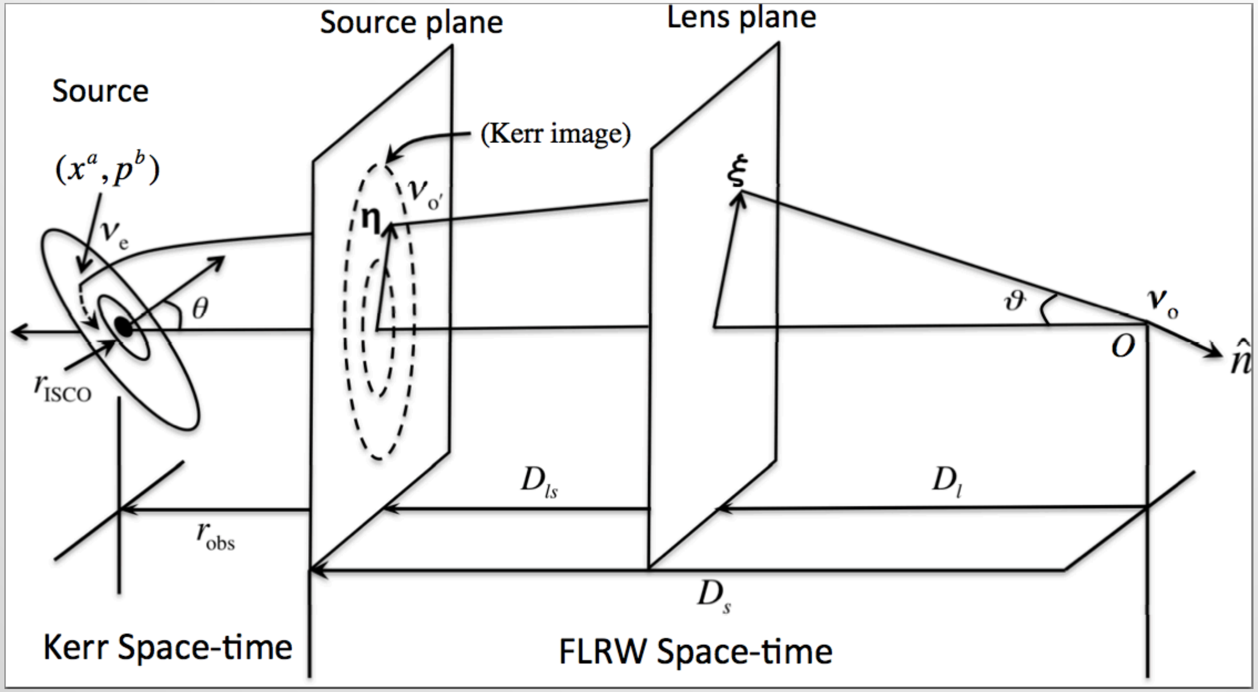

Chen et al. (2013)

- Ray Tracing Model for Kerr Space-time
- Macro lens model
- Micro model

KErr Ray-Tracing And Polarization (KERTAP, Chen et al. 2015)

- Python/Cython Code
- Parallel Code (support Mpirun or OpenMpI)
- Public Code

a = 0.998, i = 75 deg

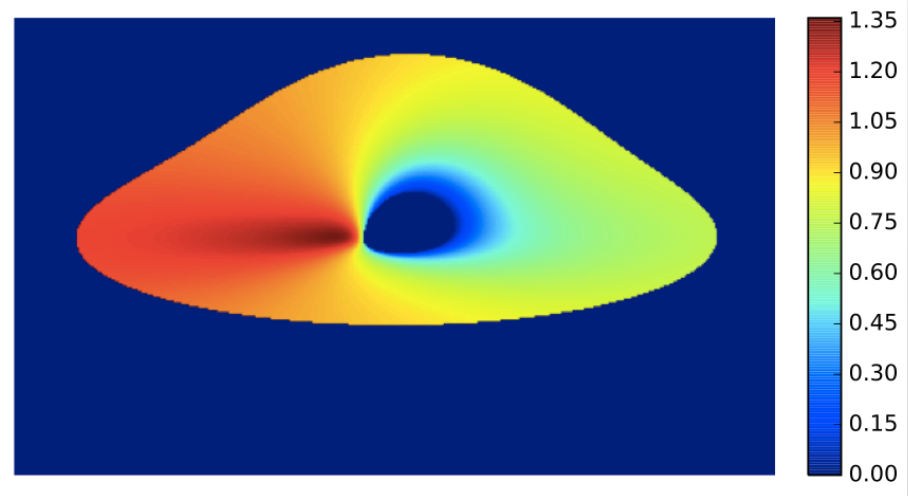

g-image

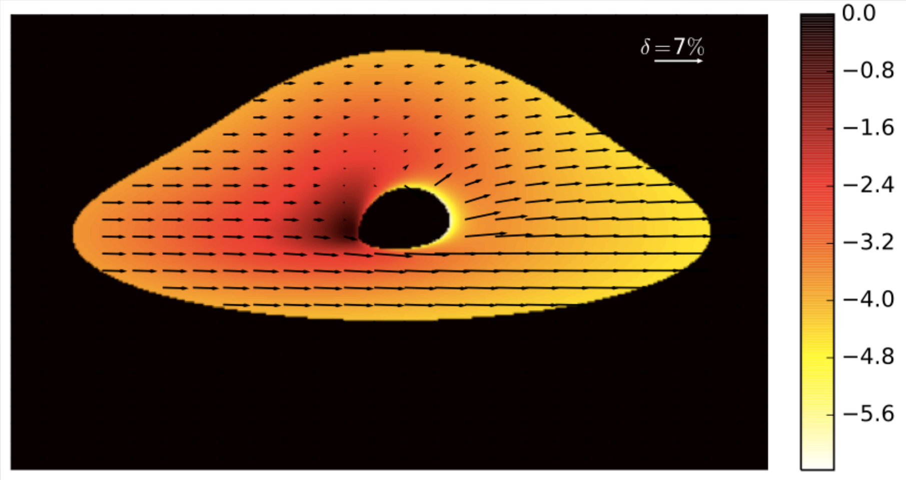

polarization-image

Excess of Iron Line Equivalent Width in Lensed Quasars (Microlensing Effect I)

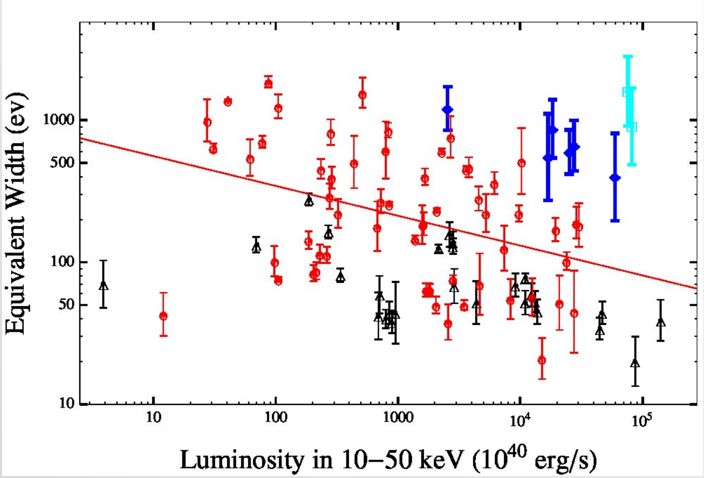

Chen et al. (2012)

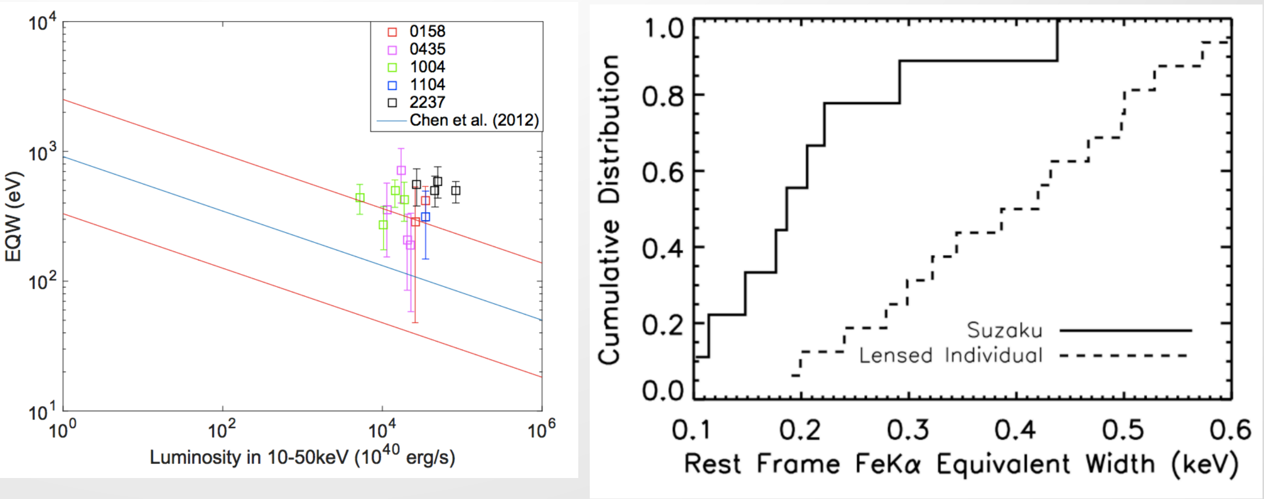

Dai, Steele, Guerras, Morgan, Chen (2019)

- Iron line EWs in lensed quasars are larger than those of normal AGN of same luminosities.
- Iron line size is even smaller than X-ray continuum.

Microlening Analysis of Excess of Iron Line EQW

- r^{-n} image profiles
- Inclination is set to 40 deg
- Spin from 0 to 0.998
- n from 2.5 (fixed for continuum) to 6.2
- Kerr raytrace region 60 r_g

- 16k x 16k microlensing maps
- Pixel size: 0.6 r_g

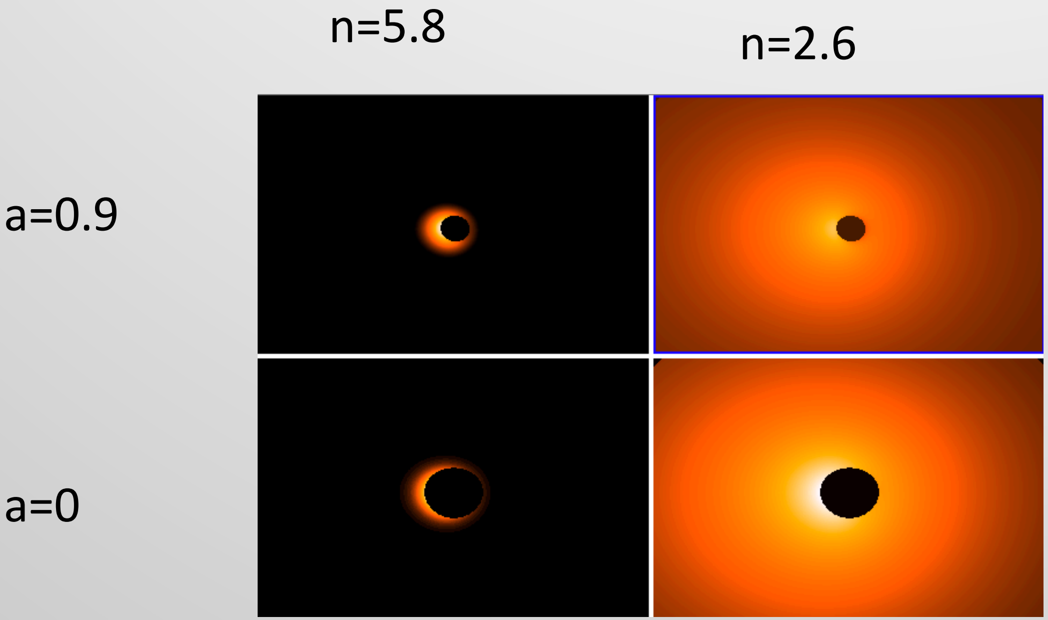

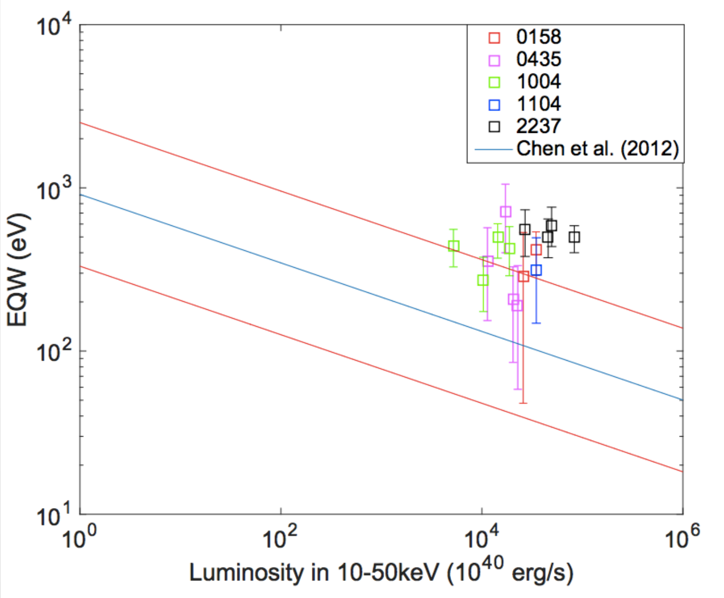

Convolved Differential Microlensing Histograms

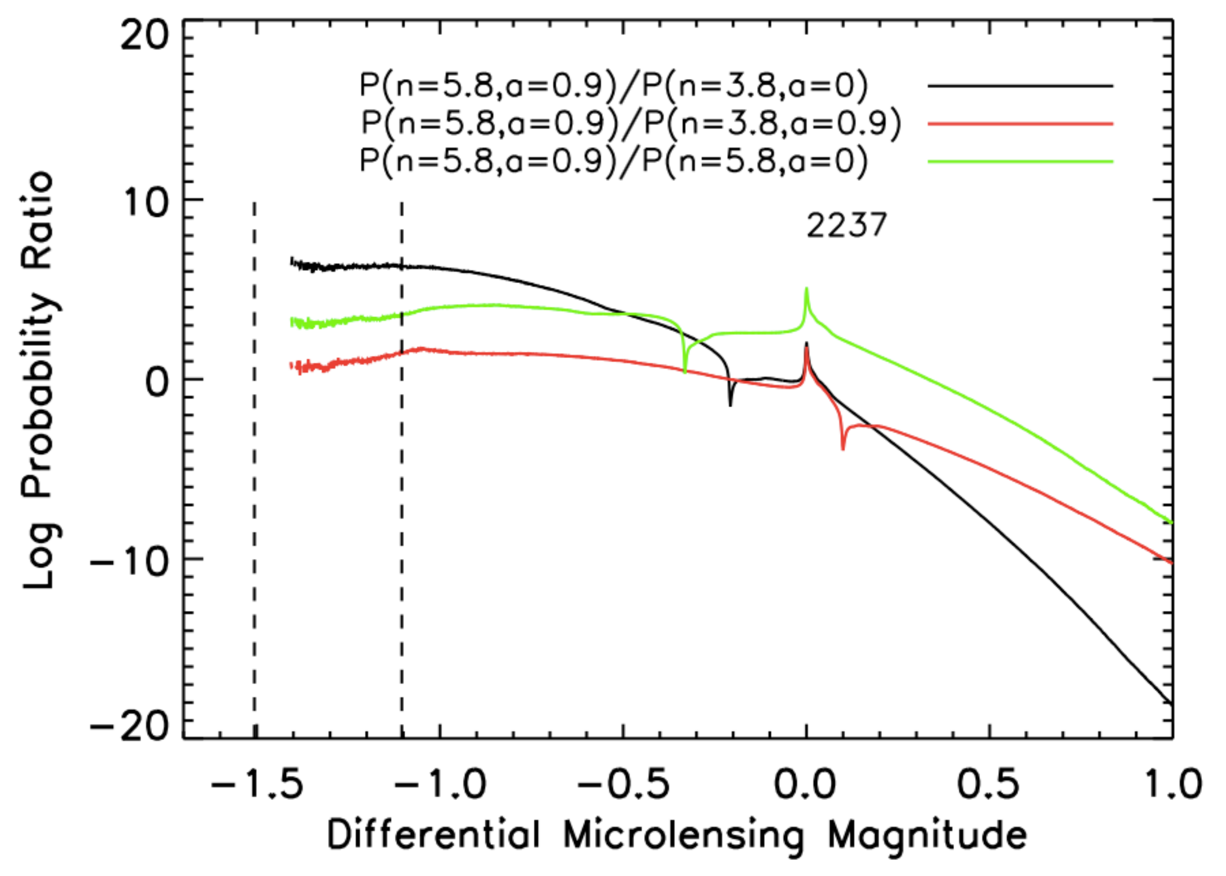

For Q2237A

Constraints on Black Hole Spins

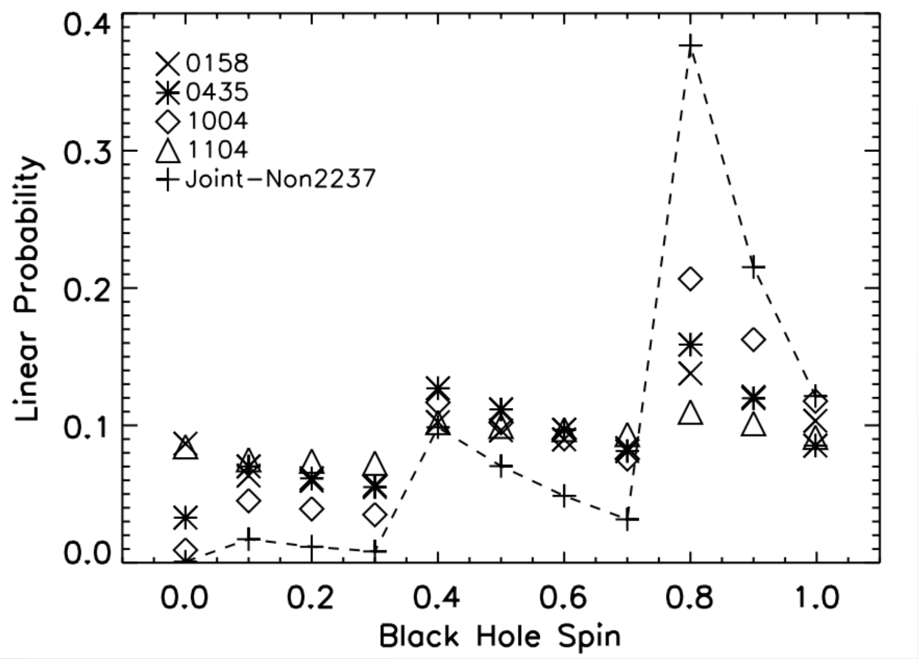

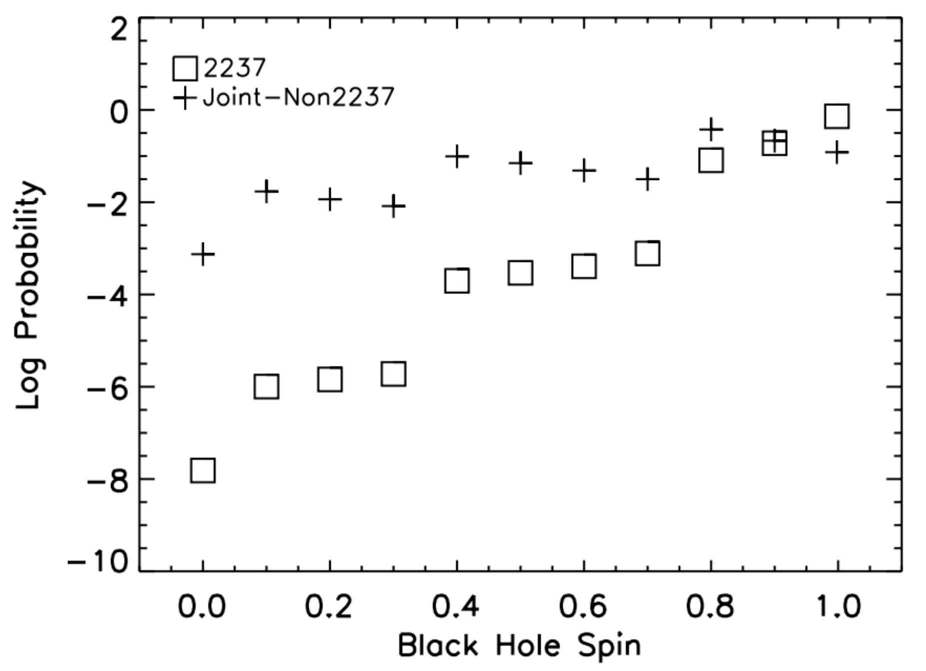

a = 0.8±0.16 (68%)
For the joint sample
excluding Q2237

a > 0.92 (68%) for
Q2237

Spin-Emissivity index Confidence Contour

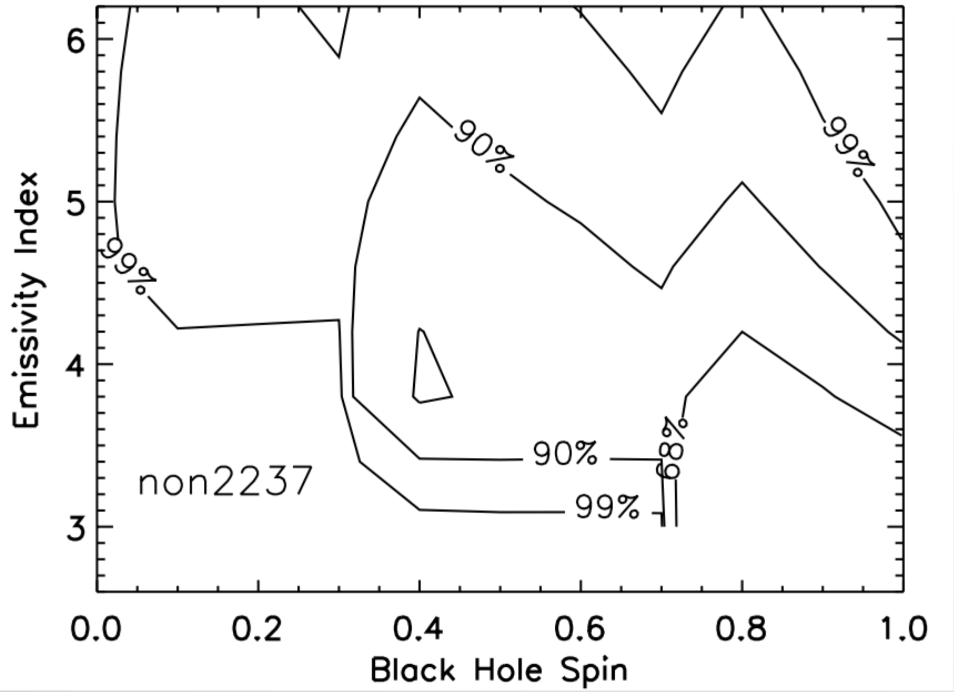

For the joint sample excluding Q2237

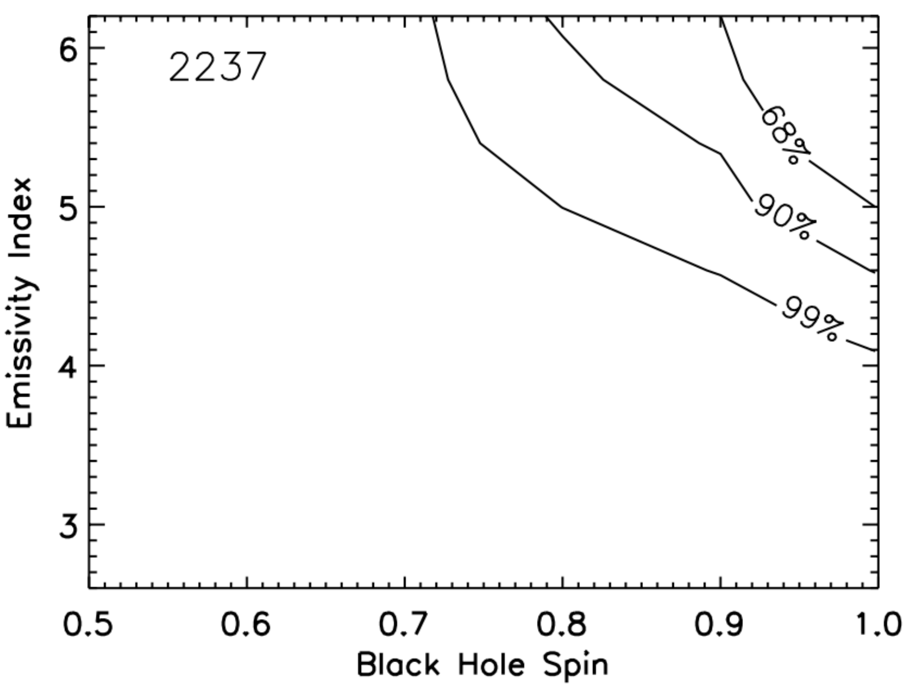

Q2237

g-Distribution of Line Centroids of RXJ1131 (Microlensing Effect II)

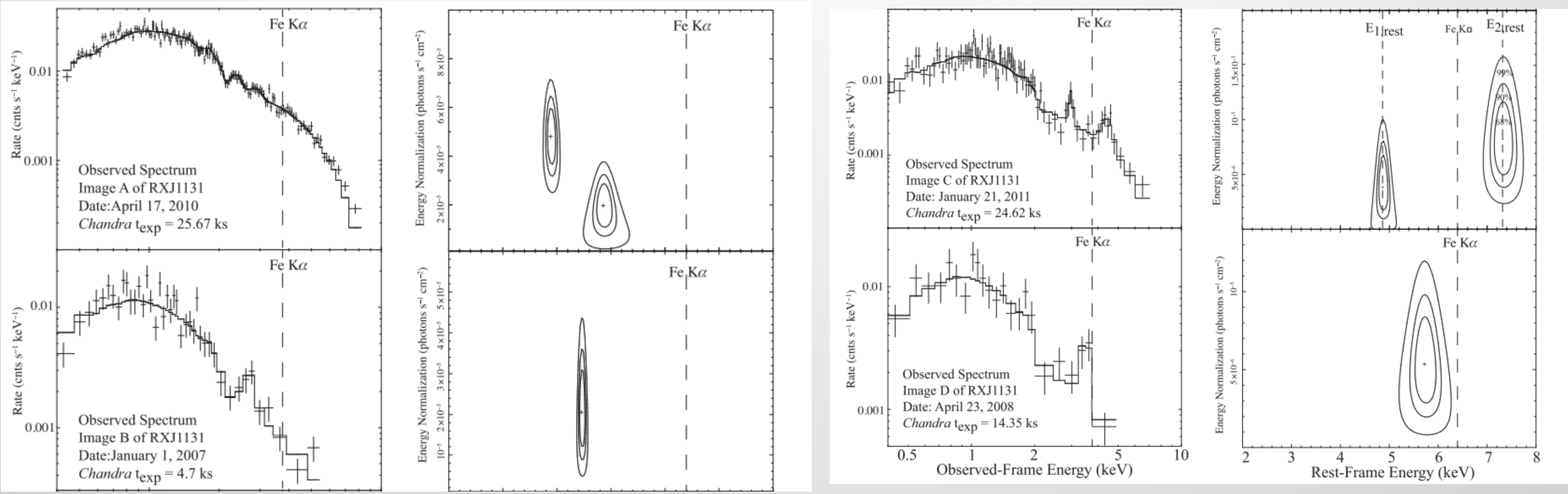

Chartas et al. 2017

g-Distribution of Line Centroids of RXJ1131 (Microlensing Effect II)

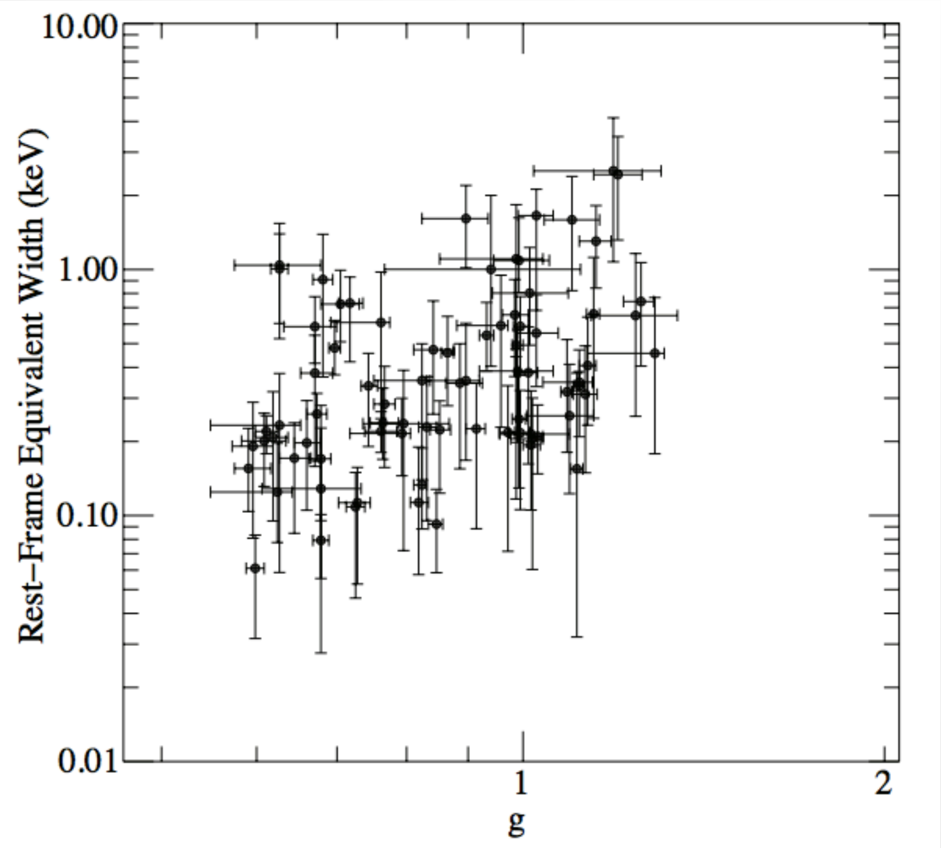

Chartas et al. 2017

a = 0.6\pm0.1 (Chartas, private communication)

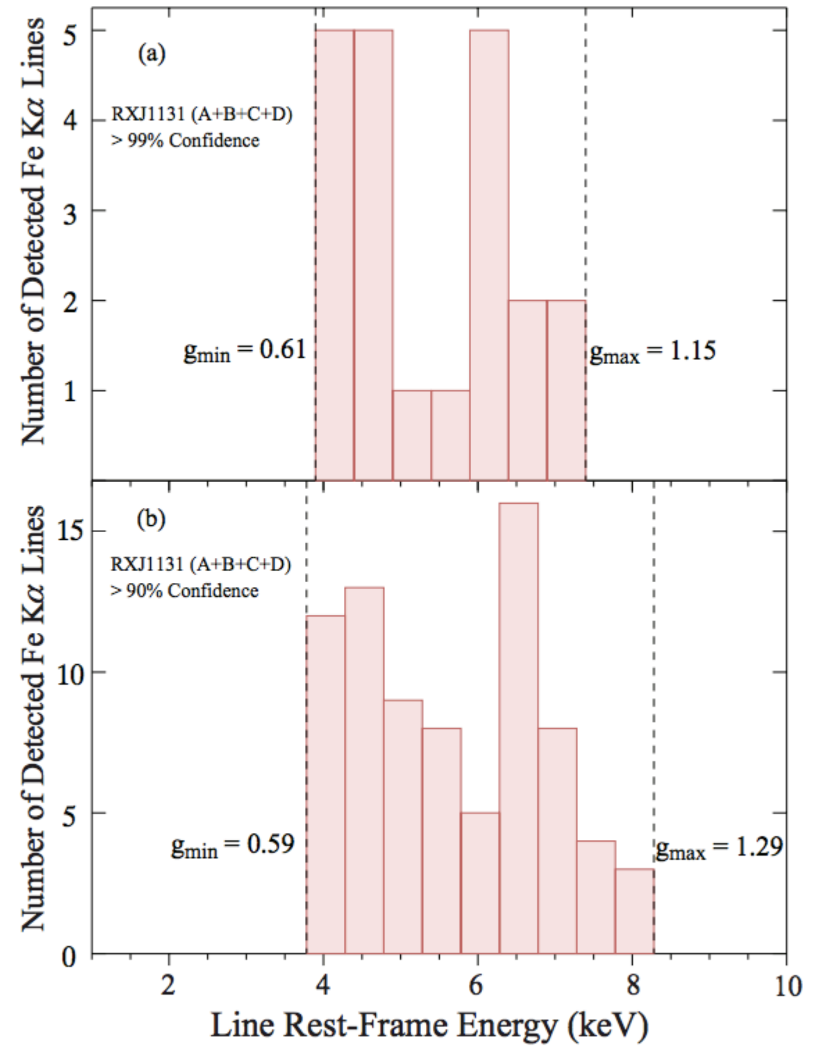

X-ray Emission of Radio-Loud Quasar

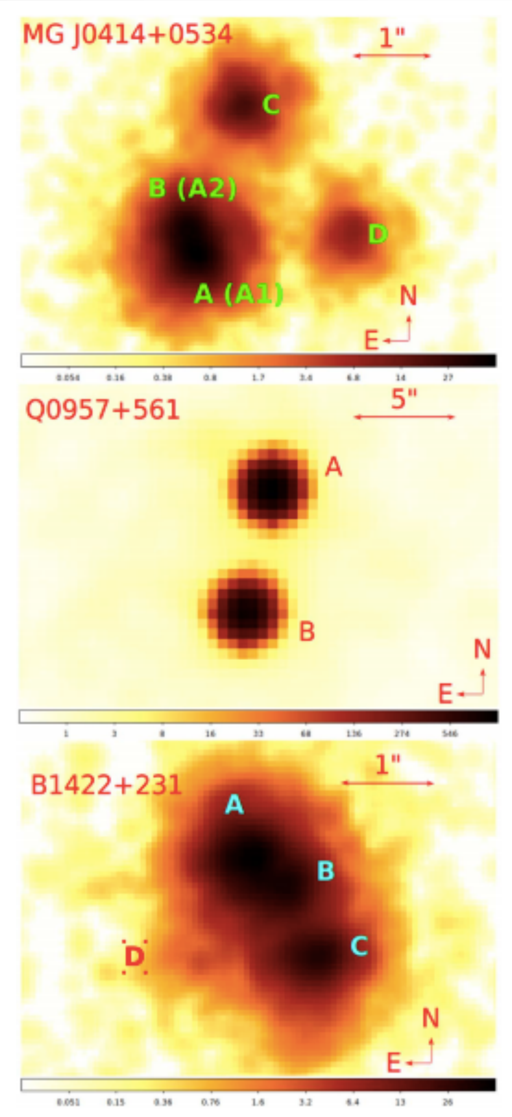

Distinguishing Jet vs. Corona emission for RL Quasars.

Constrain emission size

Dogruel et al. (2020), ApJ, 894, 153

Microlensing Fits to RL Quasars

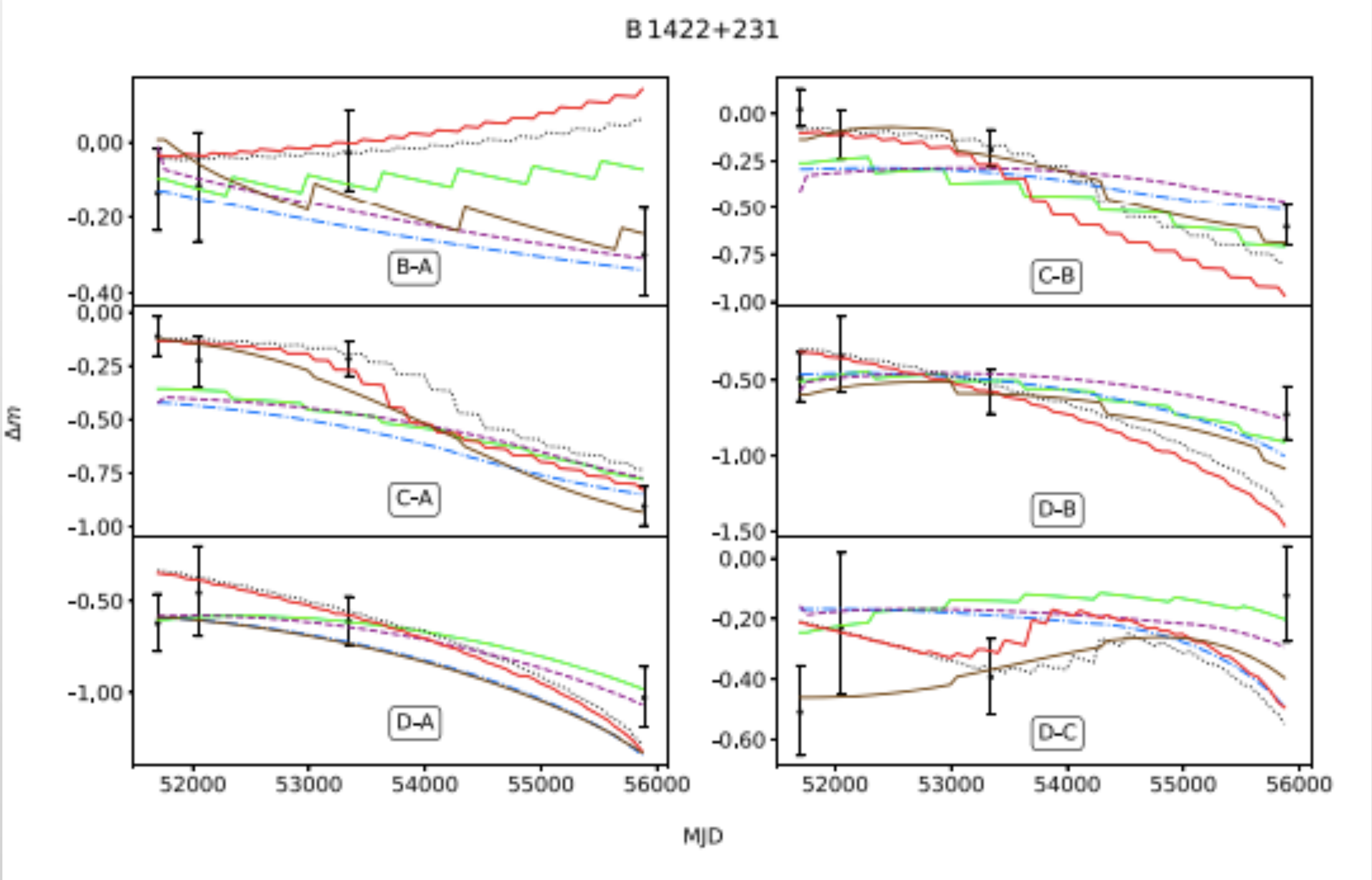

X-ray emission size is constrained to 6-12 Rg.
A compact emission size just like radio-quiet quasars.

Degenerate Results for two other RL lenses

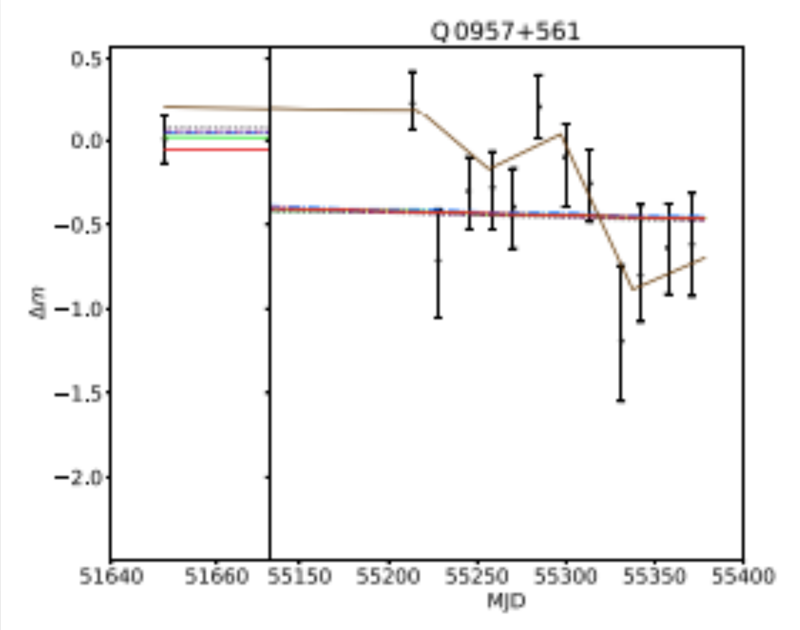

Bayesian: 130 Rg
Maximum Likelihood: 2 Rg

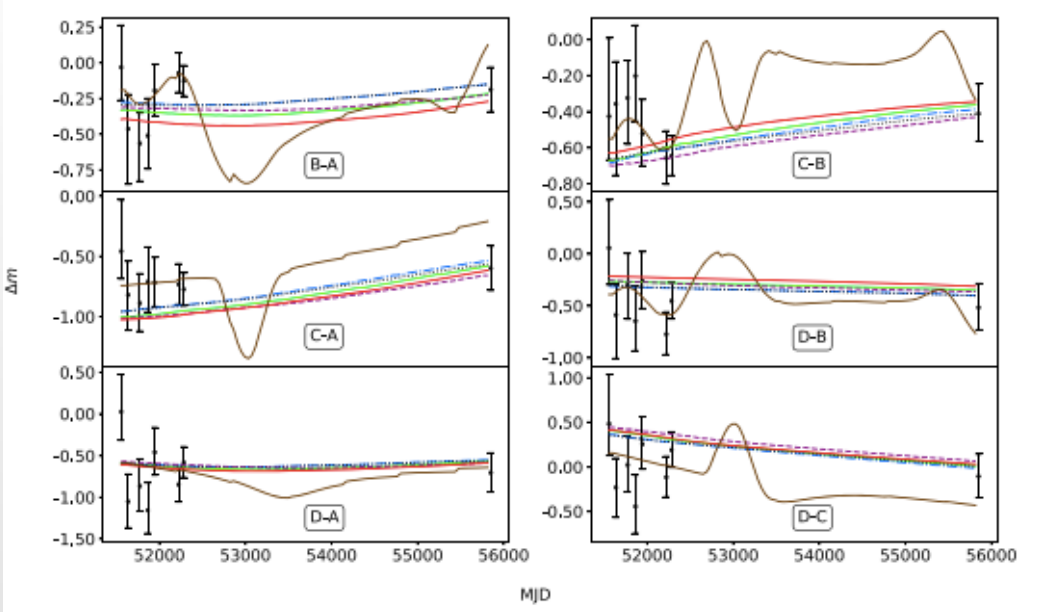
MG0414+0534

Bayesian: 60 Rg
Maximum Likelihood: 16 Rg

X-ray emission Size of RL Quasars

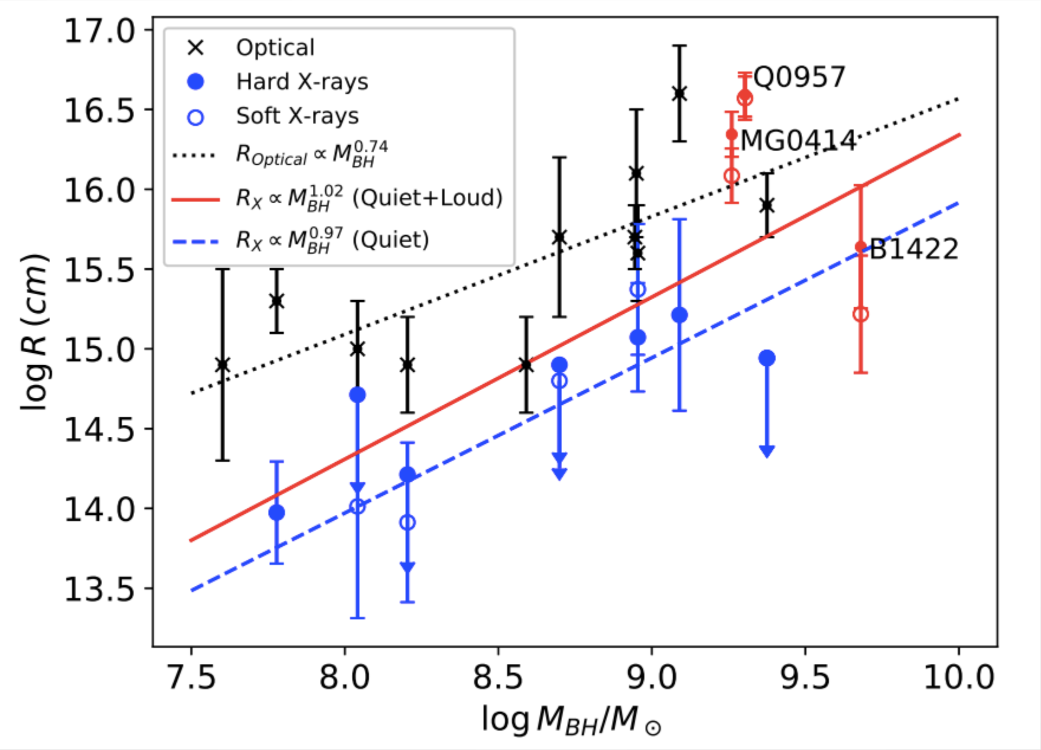

New observations of MG0414, PKS1830-211, and B1152+199 are approved to improve the radio-loud sample.

Dogruel et al. (2020),
ApJ, 894, 153

Measurement of Gravitational Faraday Rotation (Future Polarization Missions)

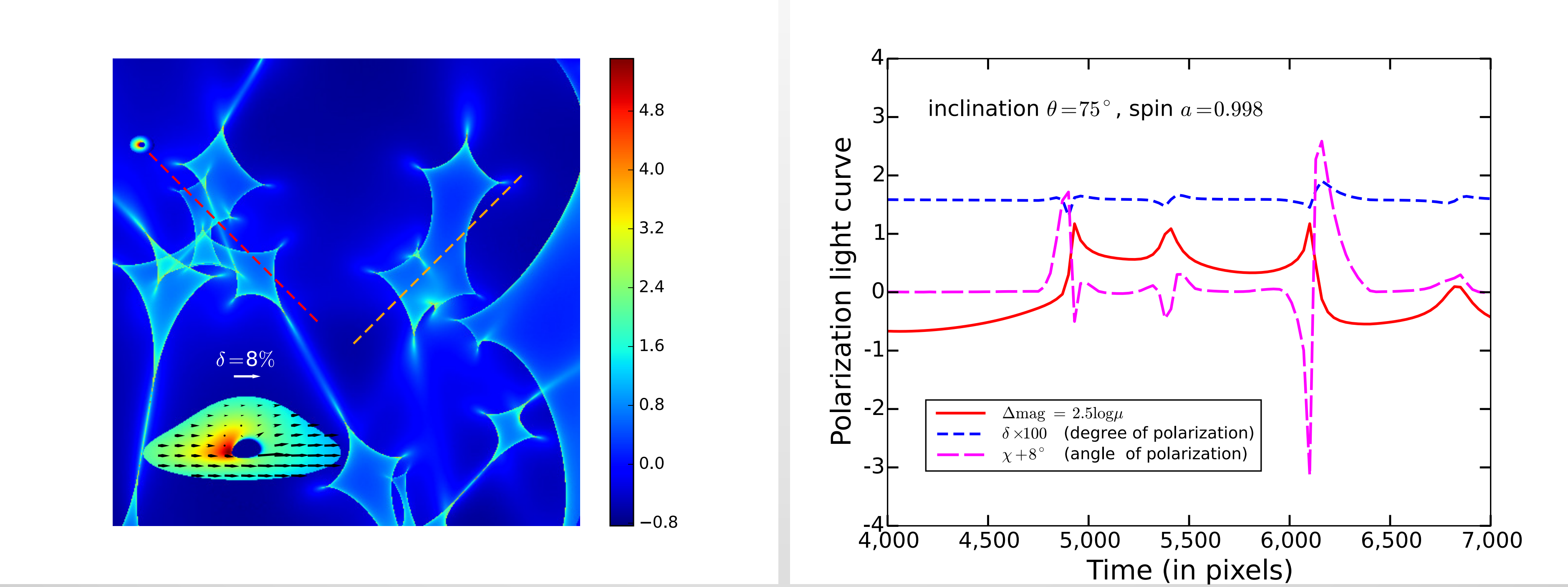

B. Chen 2015

Model of AGN Accretion Disk

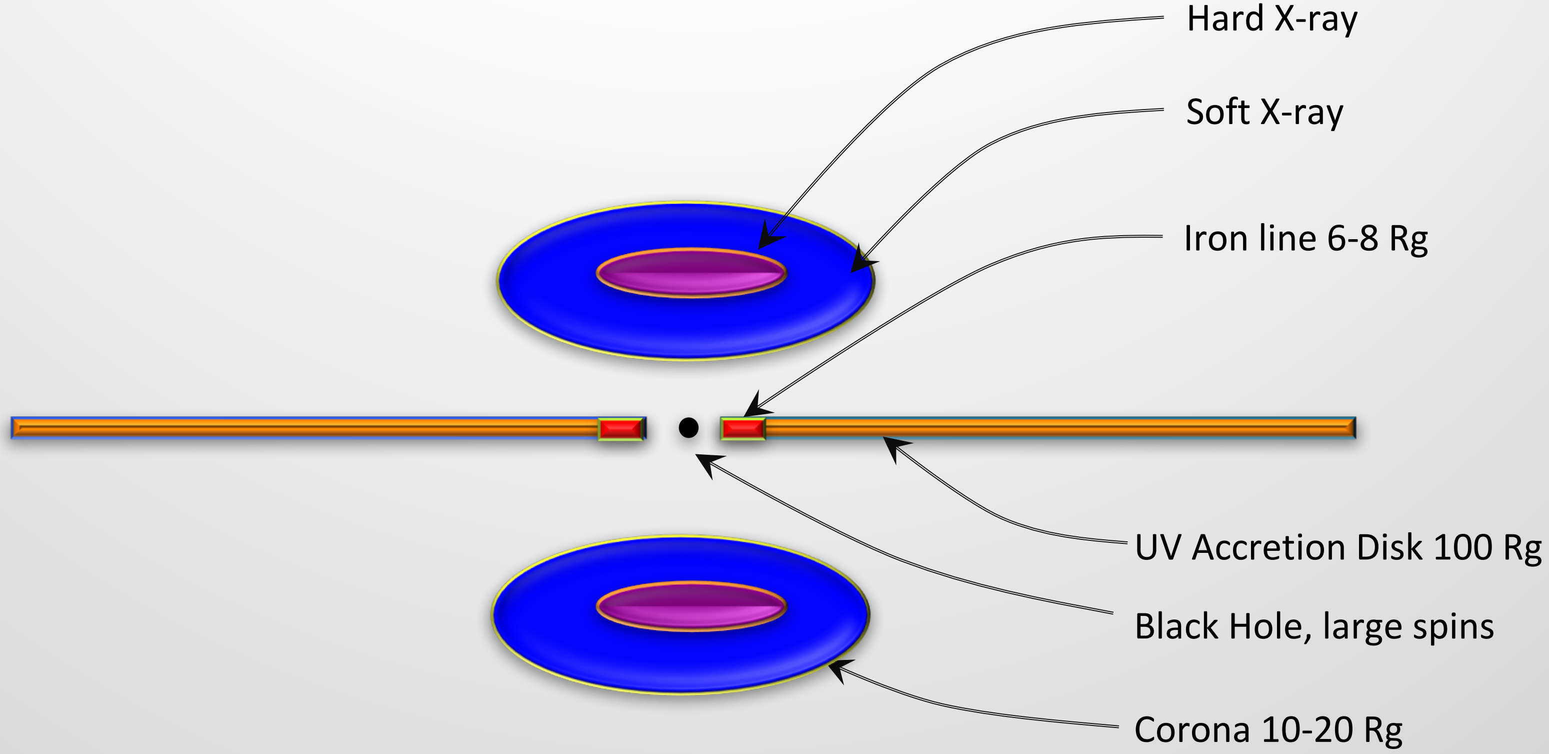

Hard X-ray

Soft X-ray

Iron line 6-8 Rg

UV Accretion Disk 100 Rg

Black Hole, large spins

Corona 10-20 Rg

Lens Population

Bhatiani’s talk